THE EFFECT OF CHOLESTEROL ON THE PARTITIONING OF 1-OCTANOL INTO POPC VESICLES

by

Roja Zakariaee Kouchaksaraee
B.Sc., Sharif University of Technology, 2004

THESIS SUBMITTED IN PARTIAL FULFILLMENT OF
THE REQUIREMENTS FOR THE DEGREE OF

MASTER OF SCIENCE

In the
Department of Physics

© Roja Zakariaee Kouchaksaraee 2009

SIMON FRASER UNIVERSITY

Summer 2009

APPROVAL

Name: **Roja Zakariaee Kouchaksaraee**

Degree: **Master of Science**

Title of Thesis: **The Effect of Cholesterol on the Partitioning of 1-Octanol into POPC Vesicles**

Examining Committee:

          Chair: **Dr. J. Steven Dodge**
Associate Professor of Physics

_____

Dr. Barbara Frisken
Senior Supervisor
Professor of Physics

_____

Dr. Jenifer Thewalt
Supervisor
Professor of Physics

_____

Dr. Martin Zuckermann
Supervisor
Adjunct Professor of Physics

_____

Dr. Nancy Forde
Internal Examiner
Assistant Professor of Physics

Date Defended/Approved: July 06, 2009

ABSTRACT

Microcalorimetry has become a method of choice for sensitive characterization of biomolecular interactions. In this study, isothermal titration calorimetry (ITC) was used to measure the partitioning of 1-octanol into lipid bilayers composed of 1-palmitoyl-2-oleoyl-sn-glycero-3-phosphocholine (POPC), a semi-unsaturated lipid, and cholesterol, a steroid, as a function of cholesterol molar concentration. The ITC instrument measures the heat evolved or absorbed upon titration of a liposome dispersion, at concentrations ranging from 0 to 40% cholesterol, into a suspension of 1-octanol in water. A model function was fit to the data in order to determine the partition coefficient of octanol into POPC bilayers and the enthalpy of interaction. I found that the partition coefficient increases and the heat of interaction becomes less negative with increasing cholesterol content, in contrast to results found by other groups for partitioning of alcohols into lipid-cholesterol bilayers containing saturated lipids. The heat of dilution of vesicles was also measured.

Keywords: Partition coefficient; POPC; 1-Octanol; Cholesterol; Isothermal titration calorimetry; Lipid-alcohol interactions

Subject Terms: Calorimetry; Membranes (Biology); Biophysics; Biology -- Technique; Bilayer lipid membranes -- Biotechnology; Lipid membranes -- Biotechnology

EXECUTIVE SUMMARY

Model membranes have been studied extensively in order to learn about various properties and aspects of biological cell membranes. Biological cell membranes are constructed from lipids and various proteins. The major lipids in the cell membranes are phospholipids. Cholesterol is also present in significant amounts in most cell membranes of animals and plants. Therefore, in this project, vesicles consisting of a mono-unsaturated phospholipid, 1-palmitoyl-2-oleoyl-sn-glycero-3-phosphocholine (POPC), and cholesterol were used as the model membranes.

The means by which anesthetic molecules impact cell behaviour have been probed during the past decades. However, the exact mechanism is not yet completely known and more research is being conducted attempting to explore the interaction of anesthetics with cell components and their effects on cell functions. Motivated by these investigations, this project examined the partitioning of an anesthetic alcohol, 1-octanol, into the bilayers of POPC-cholesterol at molar concentrations ranging from 0 to 40% cholesterol.

POPC and cholesterol in the desired ratios were first dissolved in a solvent and lyophilized. The lyophilized solid remnant was then hydrated and mixed, using the freeze-thaw-vortex process, in order to guarantee a well-mixed and uniform mixture. The lipid dispersions were made at the nominal concentration of 20 mM. The large unilamellar vesicles (LUVs) were produced

using several extrusions of the lipid dispersion through two stacked 100 nm filters.

The main technique used in this study was the so-called "gold standard" for measurements of binding and partitioning of macromolecules, isothermal titration calorimetry (ITC). The ITC instrument, MSC_ITC, measures the heats generated or absorbed during the injection of one reactant (the lipid dispersion) into the other (octanol:water suspension) using the power compensation method. This highly sensitive microcalorimetry technique allows accurate determination of different thermodynamic parameters such as enthalpy, entropy and other parameters such as binding or partitioning constants. In this work, the ITC technique was used to measure the partitioning of 1-octanol into the POPC bilayers containing cholesterol at temperature of 45°C. Using a model function, the ITC data were analyzed and the partition coefficient and the enthalpy of interaction were evaluated. The heats of dilution of lipid vesicles in water were also determined from the fits.

The results of fitting the ITC data for the samples of different molar ratios of POPC and cholesterol in the bilayer revealed that the partition coefficient of 1-octanol into POPC bilayers increases with increasing cholesterol content and the enthalpy of interaction becomes less negative. These results are different from those for saturated lipids, for which the partition coefficient of different alcohols decreases with addition of cholesterol and the enthalpy of interaction changes from a negative value for pure lipid to positive values for lipid-cholesterol mixtures.

To summarize the structure of this thesis, Ch. 1 provides an overview of the chemical backgrounds, conformations and properties of the materials used. The model function that was fit to the ITC data is also presented in this chapter. Chapter 2 describes the methods, instruments, and experiments of extrusion and ITC in detail. Chapter 3 contains the results and analysis and Ch. 4 discusses the results of this study and those of related studies reported in the literature and also the comparison of another fit function with our slightly improved function, both within the same model. Finally, Ch. 5 concludes the thesis and presents further possible directions to follow in this project.

To my loving husband, Damon

ACKNOWLEDGEMENTS

TABLE OF CONTENTS

LIST OF FIGURES

LIST OF TABLES

CHAPTER 1:
LIPIDS, ALKANOLS AND ISOTHERMAL TITRATION CALORIMETRY

In this chapter, the materials and methods used in this work will be introduced. Different categories of lipids, their molecular structures and properties are presented, including two lipids used in this study: POPC and cholesterol. In addition, a brief introduction to the method of isothermal titration calorimetry (ITC) is given. The theoretical background and the model used in the data analysis are also discussed.

1.1 Lipids: Classification, Structure and Properties

Lipids are one of the major chemical organic substances that are well known for their presence in biological environments. Lipids are classified by their solubility; they are defined as substances of biological origin that are highly soluble in nonpolar organic solvents and only sparingly soluble in nonpolar solvents like water [1,2]. This definition includes fats, some hormones and vitamins, and many other substances of diverse chemical identity [2]. Chemists have divided lipids into two main classes: complex and simple lipids. Complex lipids that are easily hydrolyzed to simpler components are esters of long-chain carboxylic acids, called fatty acids. Simple lipids are those that do not undergo hydrolysis, such as steroids and prostaglandins.

1.1.1 Fatty Acids and Phospholipids

Fatty acid esters consist of two major groups: waxes and glycerides. Glycerides are fatty acids with a backbone of glycerol (glycerine), or 1,2,3-propanetriol, shown in Fig. 1.1(a). The most famous group of glycerides are triglycerides (triacylglycerols), in which all three hydroxyl, $-OH$, bonds are esterified by fatty acids [1], as shown in Fig. 1.1(b). If all three fatty acids are the same, the triacylglycerol is called a simple triglyceride, and if the fatty acids are different, it is called a complex triglyceride. Triglycerides are also known by the common terms fats or oils, depending on their state. Fats and oils are the main form of stored energy in plants, animals and humans.

(a)   **(b)**

Glycerol   Triglyceride
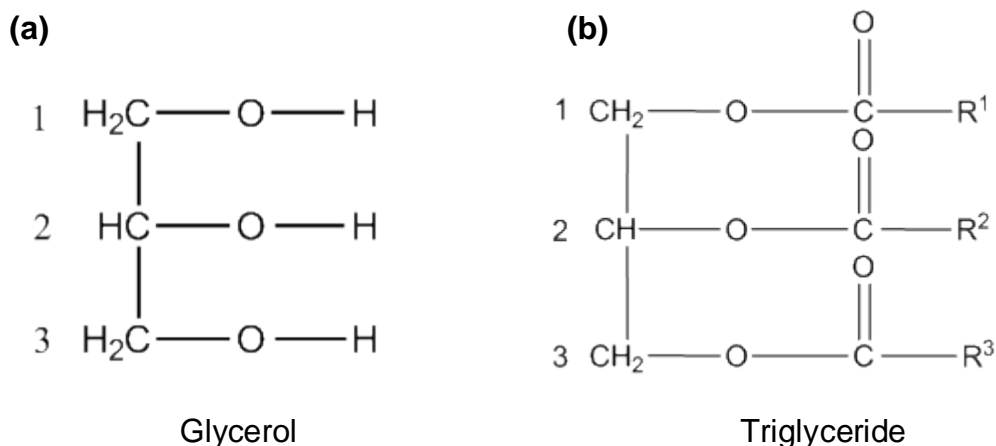
Figure 1.1 **Molecular structures of (a) glycerol and (b) triglycerides. Triglycerides are glycerol esterified by fatty acids. Symbol R is used as a substituent, normally an alkyl group.**

Fatty acids present in most triglycerides are carboxylic acids of unbranched long-chains of 12 to 20 carbon atoms. These fatty acids are divided into saturated and unsaturated groups, depending on their carbon-carbon bonds. Saturated lipids only contain single bonds, whereas unsaturated lipids contain

one or more carbon-carbon double bonds. A lipid is called di-monounsaturated if its two acyl chains are monounsaturated, and is called polyunsaturated if there is more than one double bond in a given hydrocarbon chain. Some of the common saturated and unsaturated fatty acids that exist as triglycerides and that are mentioned later are illustrated in Table 1.1 [1].

Name	Carbons	Molecular Structure
Saturated		
myristic acid	**14**	COOH
palmitic acid	**16**	COOH
stearic acid	**18**	COOH
Unsatu-rated		
oleic acid	**18**	COOH
linoleic acid	**18**	COOH

Table 1.1   Structure of some common saturated and unsaturated fatty acids, mentioned in this study (adapted from [1]).

Lipids that contain groups derived from phosphoric acid are called phospholipids. As it will be discussed in Ch. 4, phospholipids are known to be the major element of biological membranes. They are divided into two main groups: glycerophospholipids (phosphoglycerides) and sphingophospholipids. Phosphoglycerides are the most common class of phospholipids because they are the principal phospholipids in biological tissues [3]. Phosphoglycerides are

lipids in which a phosphoric acid group replaces one of the fatty acids in a triglyceride. If the two other chains remain as fatty acids they are called phosphatidic acids, the simplest class of phosphoglycerides, as shown in Fig. 1.2(a) [1].

(a)

1 CH_2—O—C(=O)—$(CH_2)_n$ CH_3

2 CH—O—C(=O)—$(CH_2)_m$ CH_3

3 CH_2—O—P(=O)—OH

OH

A typical phosphatidic acid

(b)

1 CH_2—O—C(=O)—$(CH_2)_n$ CH_3

2 CH—O—C(=O)—$(CH_2)_m$ CH_3

3 CH_2—O—P(=O)—O—CH_2CH_2—$N^+(CH_3)_3$

O^-

Phosphatidyl choline

(c)

polar head   nonpolar hydrocarbon tails
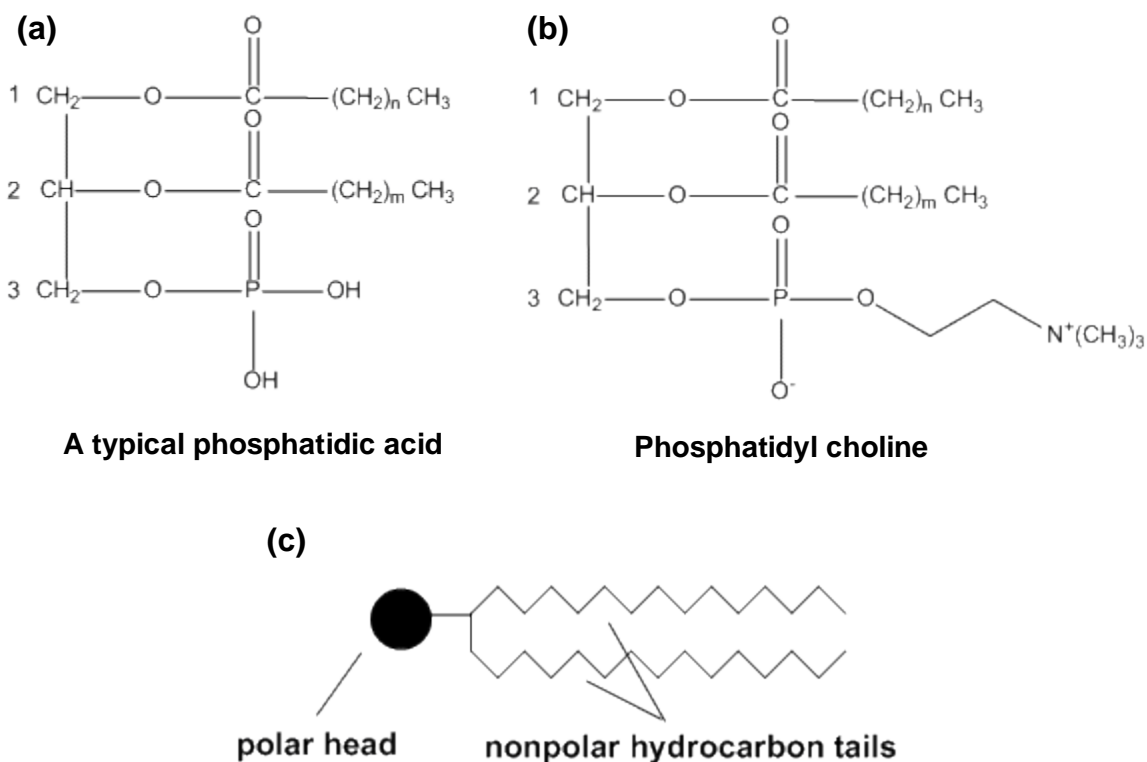
Figure 1.2   Molecular structures of (a) phosphatidic acid and (b) lecithin or phosphatidyl choline. (c) The schematic illustration of a phospholipid, with indication of its polar and nonpolar parts.

Different types of phosphatidic acids depend on the group by which the phosphate is esterified, such as an additional alcohol. Lecithins or phosphatidyl cholines are the corresponding esters of choline, an alcohol with molecular structure of $HO - CH_2CH_2 - N^+(CH_3)_3$, illustrated in Fig. 1.2(b). As shown in Fig. 1.2(c), phospholipids have a polar headgroup, such as the phosphatidyl-choline group, and two nonpolar tails, the fatty acids. The polar head is

hydrophilic, or water-loving, and the nonpolar tails are hydrophobic, or water-hating. These types of molecules with this dual nature are called amphiphilic molecules. Since the strong attractive forces between water molecules (the hydrogen bonds) make them isotropically arranged, any disruption or distortion to this arrangement by solute molecules leads to a drop in the entropy of the water molecules. Polar solutes form new hydrogen bonds with water molecules that compensate this loss. However, in the case of nonpolar solutes, no such compensation occurs and their solubility in water is accordingly poor, i.e. the loss of entropy leads to an unfavourable free energy change of the solution process [2]. Therefore, when lipid molecules are dispersed in water they form aggregates, of the shapes including those illustrated in Fig. 1.3, so that the polar headgroups are exposed to water, making the hydrogen bonds, and the nonpolar hydrocarbon tails are shielded inside. These aggregates are soluble in water and are energetically more favourable. Examples of amphiphilic molecules include surfactants and lipids. Lipids with double chains mostly aggregate as either planar bilayers or vesicles, Fig 1.3 (a) and (b), while those with single chains normally associate into micelles, Fig. 1.3 (C) [4].
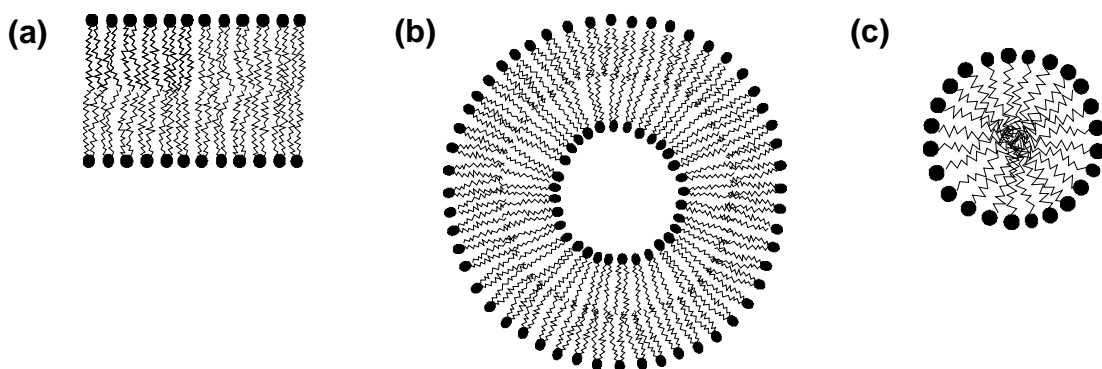
Figure 1.3   Different possible self-assembly structures of lipid molecules in an aqueous environment: (a) planar bilayer, (b) vesicle, and (c) micelle.

The nomenclature of the phosphatidyl choline lipids is based on the associated fatty acids. The main lipid used in this study was a phosphatidyl choline called 1-palmitoyl-2-oleoyl-*sn*-glycero-3-phosphocholine (POPC), with the molecular structure shown in Fig. 1.4. The carbons of the glycerol backbone are numbered, since the nomenclature originates from the groups connecting to each carbon. The first carbon is attached to the ester of the palmitic acid, i.e. palmitoyl, the second carbon is bonded to the ester of oleic acid, i.e. oleoyl, and the third carbon is bonded to the phosphatidylcholine group. Palmitic acid is saturated, while oleic acid is mono-unsaturated containing a *cis* double bond between its ninth and tenth carbons. Therefore, POPC is a mono-unsaturated phospholipid.
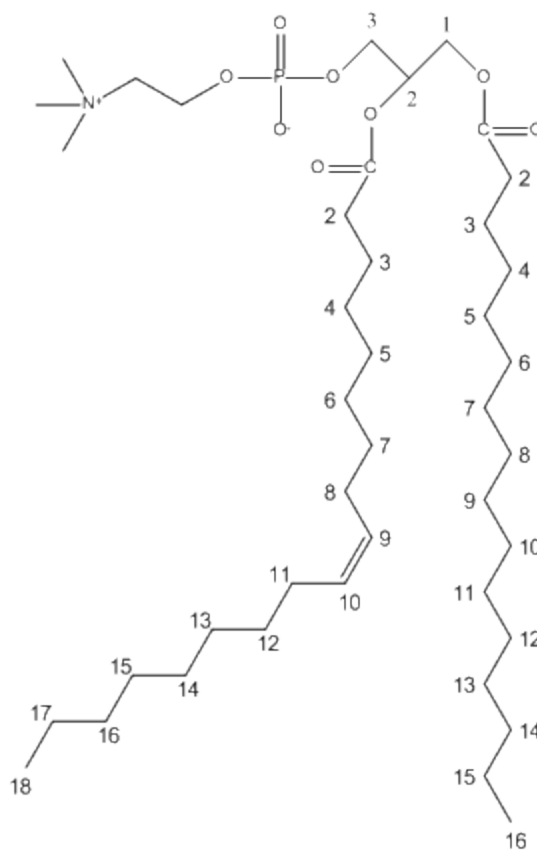
Figure 1.4   The molecular structure of POPC. The first carbon of the glycerol backbone is bonded to saturated 16-carbon palmitic acid. The second carbon is bonded to 18-carbon mono-unsaturated oleic acid, which has one *cis* double bond between C9 and C10.

Other phosphatidylcholines that are very common and are seen in similar studies are DMPC and DPPC, with molecular structures of 1,2-dimyristoyl-*sn*- 3-glycero-phosphocholine and 1,2-dipalmitoyl-*sn*-3-glycero-phosphphocholine, respectively. The schematic molecular structures of these two lipids are shown in Fig. 1.5(a) and (b). Two identical acyl chains are bonded to the first and second carbons of the glycerol backbone of these lipids: 14-carbon myristic acid in DMPC and 16-carbon palmitic acid in DPPC. This is why their molecular names contain the prefix *di-*, standing for double or two. As can be learnt from their molecular structures, these phospholipids are fully saturated and therefore both of their hydrocarbon tails are straight and unbent.
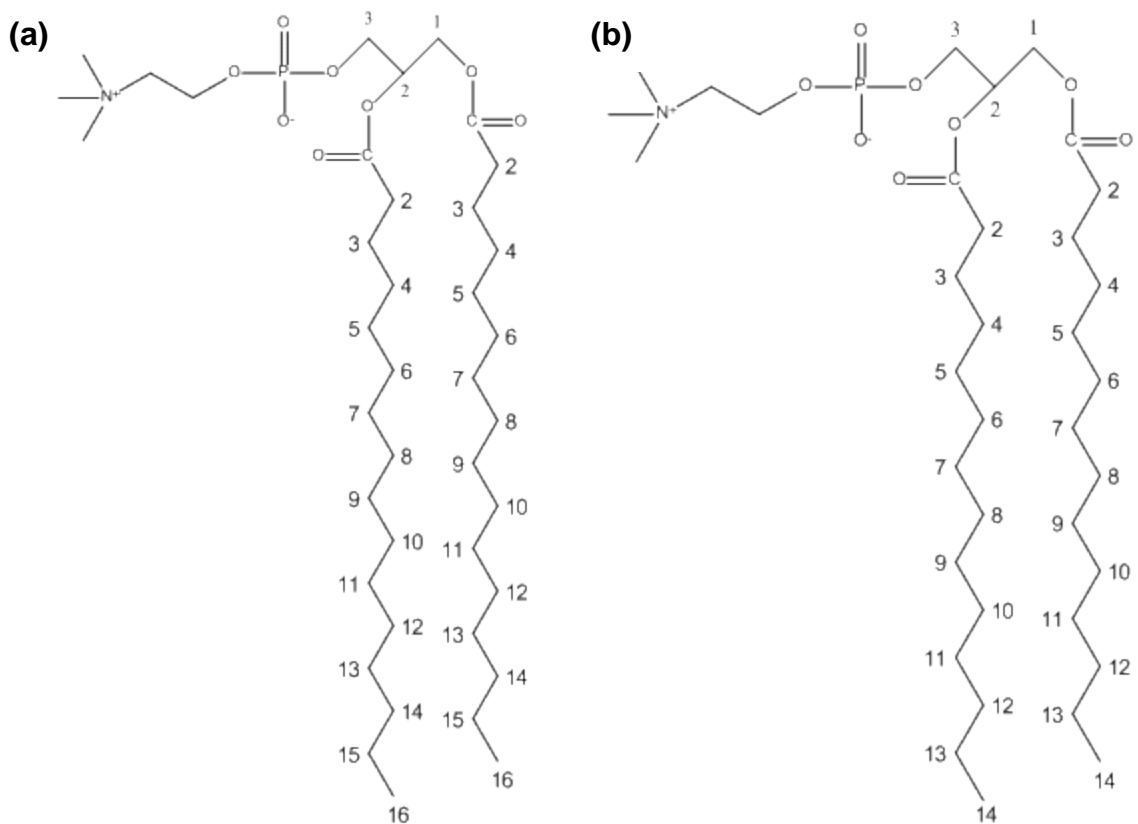
Figure 1.5 **The molecular structure of (a) DMPC and (b) DPPC. In both molecules, the first and second carbons of the glycerol backbone are bonded to two similar saturated fatty acids. DMPC contains two 14-carbon myristic acids, and DPPC contains two 16-carbon palmitic acids. Both molecules are fully saturated and have unbent hydrocarbon tails.**

Phase Behaviour

Fully hydrated phospholipid bilayers have calorimetric phase behaviour. The lipid chains undergo a well-defined thermotropic phase transition as the temperature is increased. The lipid bilayer phases that occur in the lipid membranes, in order of their occurrence at increasing temperature, are solid or ordered crystalline phase (*so)* and the fluid or liquid-disordered phase (*ld*). The *so* phase is used to describe the gel phase and, if it exists, the ripple phase. The main phase transition, also called the chain-melting transition, happens between the maximum limit of the gel phase and the fluid phase, as the temperature is raised. The temperature at which this transition occurs is called the main phase-transition temperature T_m.

Different lipids have different phase-transition temperatures, based on their characteristics such as their saturation/unsaturation status, total number of carbons, and the headgroup. The degree of unsaturation has a direct effect on the phase transition temperature, especially if the *cis* double bonds of one or two of their acyl chains cause the unsaturation. The *trans* double bonds have a smaller effect on the melting point than the *cis* bonds, because of the geometry of the *trans* double bond which is similar to the uniform zigzag conformation of a saturated hydrocarbon chain therefore it does not kink the chain as the *cis* double bond does [1]. The phase-transition temperature depends on the packing ability of the molecules, and this directly depends on the configuration of their acyl chains, i.e. whether they are straight or bent. Therefore, the phase-transition temperature of the fully saturated phospholipids is higher than that of mono-

unsaturated lipids, due to higher packing capacity of fully saturated phospholipids, which is in turn higher than that of di-monounsaturated and polyunsaturated lipids.

The chain-melting phase-transition temperature of homologous saturated phospholipids is reported to increase with the total number of carbons [4,5]. This is because intrachain melting and spatial disorder vary linearly with the number of carbons, leading to the entropy of hydrocarbon fluidization being proportional to the chain length [3].

1.1.2 Cholesterol: a Steroid

As mentioned in the previous section, one class of simple lipids is steroids. Steroids are polycyclic molecules with a cyclophenanthrene nucleus. They are present in all plants and animals and are very important physiologically as hormones, emulsifiers, and are a major component of cellular membranes [1,6].   As presented in Fig. 1.6(a), the nucleus of different steroids is cyclophenanthrene, which has four rings, labeled A, B, C, and D, whose carbon atoms are numbered as shown. The steroid alcohols may occur freely or as esters with different compound groups. The addition of two methyl groups to C10 and C13 forms the molecule androstane, as illustrated in Fig. 1.6(b). The solid wedge bond between C10 and C19, and between C13 and C18 represents the fact that the methyl group is projecting out of the page and the hashed wedge bond connecting carbons 5, 9, and 14 to the hydrogen atoms represents the fact that the hydrogens are projecting into the page [6].

9
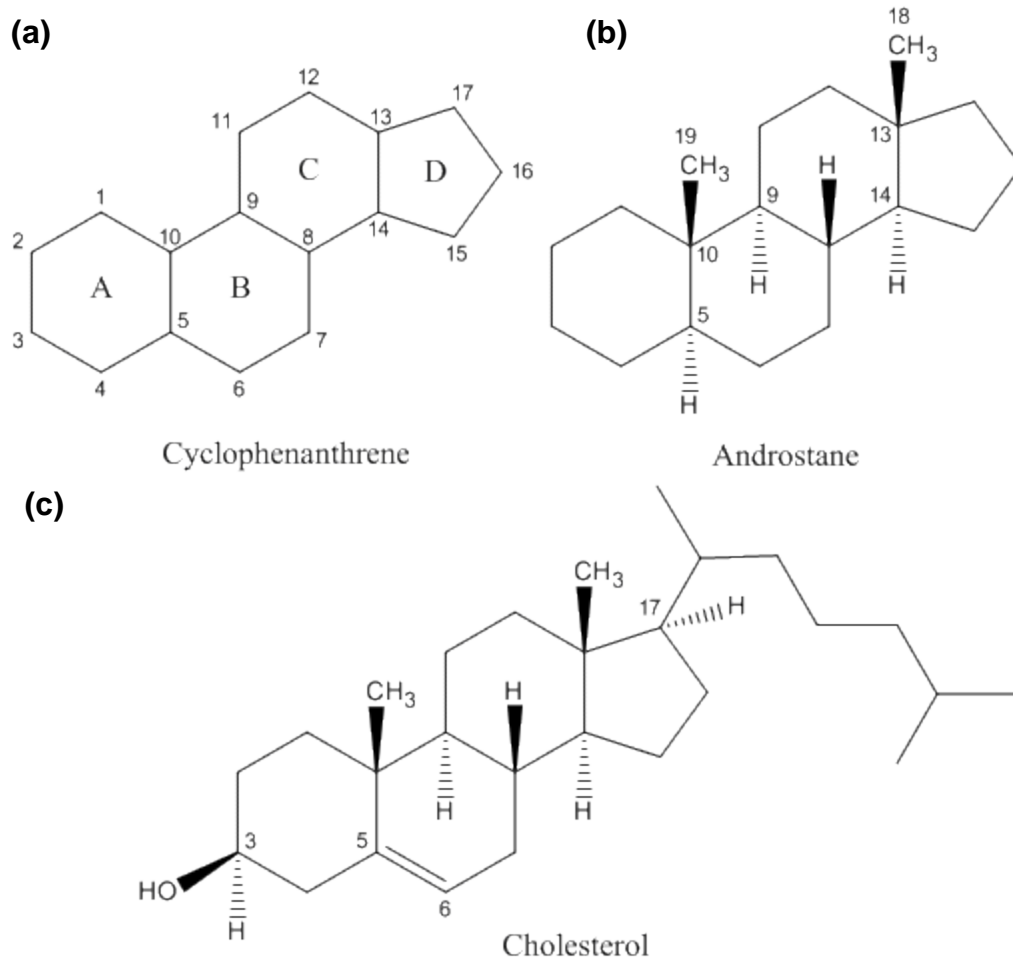
Figure 1.6 The molecular structures of (a) cyclophenanthrene, (b) androstane, and (c) cholesterol. Cyclophenanthrene is the nucleus of the steroids, whose one ester is androstane that is the nucleus of cholesterol.

Cholesterol has an androstane nucleus with an 8-carbon side chain at C17, and a double bond between C5 and C6, as shown in Fig. 1.6(c). Cholesterol is a well-studied biological intermediate molecule that is often stored in different organs such as liver, brain, adrenal and ovary. It is believed to be a biosynthetic precursor to other steroids in the body such as steroidal hormones [1,5]. It is found in the plasma membrane of mammalian cells [7] and plays a very important role in cellular membranes, modulating their fluidity, permeability, and thickness [5]. This is due to the characteristics of the lipid-cholesterol systems,

since cholesterol affects the chain packing and the gel-liquid phase transition of the lipids it is mixed with [6]. Therefore, the effect of cholesterol on the phase transition of several lipids has been extensively studied. Lipid bilayers containing cholesterol introduce a new phase, liquid ordered (*lo*), which is a kind of a gel phase [5]. In general, addition of cholesterol has been shown to reduce the main phase-transition temperature of different phospholipids and also the heat of transition [6]. The gel-liquid transition is completely removed at high cholesterol concentrations (50 mol%). A similar effect is observed in the interaction parameters of alkanols with phospholipids with varying concentration of cholesterol [8]. These subjects will be discussed in more detail in Ch. 4.

1.2 Anesthetics and n-Alkanols

The effect of some materials and plants in reducing pain has been used in surgeries and tooth extractions for a very long time. The word *anesthesia* was first used by Oliver W. Holmes in the mid-18th century [9]. While the exact mechanism by which anesthetic molecules impact living cells is not yet understood, there have been several theories suggesting different origins for the effect of anesthetics on organs. There are two standard approaches to the molecular mechanism of anesthesia: general perturbations and the specific receptor [10]. The general perturbation approach suggests that anesthetic agents disturb the normal operation of the lipid bilayer components of the cell membrane, which they are absorbed to according to the hydrophobicity of anesthetics found by Meyer-Overton [10-12]. Based on these theories, anesthetic molecules perturb the lateral pressure, fluidity, phase transitions, volume and

thickness of the lipid bilayers, and the function of some "unidentified important proteins" in the cell membrane [10]. On the other hand, the specific receptor approach, which is mostly used for local anesthetics, proposes that anesthetics act at specific sites in the cells. Theories in this traditional approach suggest that local anesthetics block conducted action potentials by their action on the sodium channels of the cells [10,13].

There is a vast diversity of materials that act as anesthetics, among which are n-alkanols, a subgroup of alcohols. Alcohol is a general term for any organic substance that has a molecular structure of $R-OH$, where R stands for the substituent of any compound which is mainly a hydrocarbon chain. There are four types of hydrocarbon compounds: alkanes, alkenes, alkynes, and aromatic hydrocarbons [1]. The difference between these groups is the carbon-carbon bonds. Alkanes contain only single bonds, alkenes contain double bonds, alkynes contain triple bonds, and aromatic hydrocarbons are in shape of a ring and are derivatives of benzene, which has three double bonds. The first three types are most common, among which alkanes are the major group. The names of alcohols consisting of these hydrocarbon chains are derived from the name of the hydrocarbon chain and the suffix –*ol* from the word "alcohol". Therefore, the corresponding alcohols are alkanols, alkenols and alkynols. Nomenclature of alkanols is based on the Greek name of the number of carbons in the longest carbon chain containing the carbon bearing the $-OH$ group, combining with the *ol* suffix, starting from methanol (n_c=1), ethanol (n_c=2), propanol (n_c=3), butanol (n_c=4), to octanol (n_c=8), nonanol (n_c=9), decanol (n_c=10) and so on. According

to the position of the $-OH$ bond, these alcohols have different properties; therefore, a general term n-alcohol is used. For example, the molecular structure of 1-alkanols is $R - CH_2 - OH$.

N-alkanols are famous for their anesthetic properties. The effect of n-alkanols on the properties of lipid membranes has been the subject of many investigations; these include the fluidity [14], phase behaviour [15], lateral pressure profiles [16], permeability [17,18], hemolysis [19], and other properties of lipid membranes [20]. The partition coefficient of different alcohols into lipid membranes has also been investigated extensively [21-24]. This subject is the main interest of this study. In Ch. 4, we will review some of the recent studies of the partitioning of n-alkanols with varying hydrocarbon chain-length into lipid membranes of different compositions. According to the literature, the chain-length of the n-alkanols is a controlling factor in their interactions with the lipid membranes.

1.3 Isothermal Titration Calorimetry

1.3.1 Introduction

Isothermal titration calorimetry (ITC) is a powerful and well-established technique that can directly measure the change of enthalpy at a constant temperature for most of the biomolecular interactions [25,26]. ITC has become the method of choice for characterizing the thermodynamics of biomolecular interactions, especially those of binding [25,27]. This is because of two main reasons: its usage does not suffer from the limitations of some other methods,

such as the constraints caused by factors such as molecular size and weight and it has several advantages over other techniques, such as its high sensitivity and exceptional ability to measure high-affinity and low-affinity interactions [25,28]. The ITC method is based on the measurement of the heat generated or absorbed during the interaction between two molecules. This provides accurate determination of reaction stoichiometry, binding constants, entropy ΔS, Gibbs free energy ΔG, etc [27,28]. The interactions of any two molecules/biomolecules can be measured using ITC technique; e.g. antigen-antibody, DNA-drug, protein-lipid, or small molecule-small molecule.

In an ITC experiment one of the reactants, the solution of a biomolecule, is titrated in small volumes (~5-10 μl), with stirring, into a reaction cell containing a second reactant. The heat released or absorbed upon their binding ΔH is monitored over time for all injections. Figure 1.7 shows representative data for a preliminary injection of 2 μl and 24 injections of 10 μl of a 20 mM POPC:water dispersion into 1.34 ml of a 4 mM octanol:water suspension taken by an ITC instrument at T=25°C. As it will be explained in detail in Ch. 2, this is the raw data of the ITC cell feedback (CFB) power that is applied to the ITC sample cell in order to maintain its temperature very close to the ITC reference cell that is kept at the desired experimental temperature. Each peak in the CFB data represents the heat change associated with the injection of a chosen volume of the sample into the ITC reaction cell. If the peaks are upward (the heat changes are positive) the interaction is endothermic, i.e. releases heat, and if the peaks are downward (the heat changes are negative) the interaction is exothermic.

The heat changes are directly proportional to the number of free solute molecules in the cell that bind or partition. The heat changes decrease as the number of free octanol molecules decrease until only the heats of dilution are being observed. Since the heat values in Fig. 1.7 are positive then the heat is absorbed upon the interaction between two reactants. The area under each peak determines the heat absorbed for that injection. A binding/partitioning curve consists of a plot of these heat values per mole of injectant against the total mole of injectant. Analysing the binding or partitioning curve with an appropriate model can yield the binding or partitioning constant, the heat of interaction and the heat of dilution. Therefore, this method is perfect for determining the partition coefficient of 1-octanol into lipid membranes, which is the scope of this study.
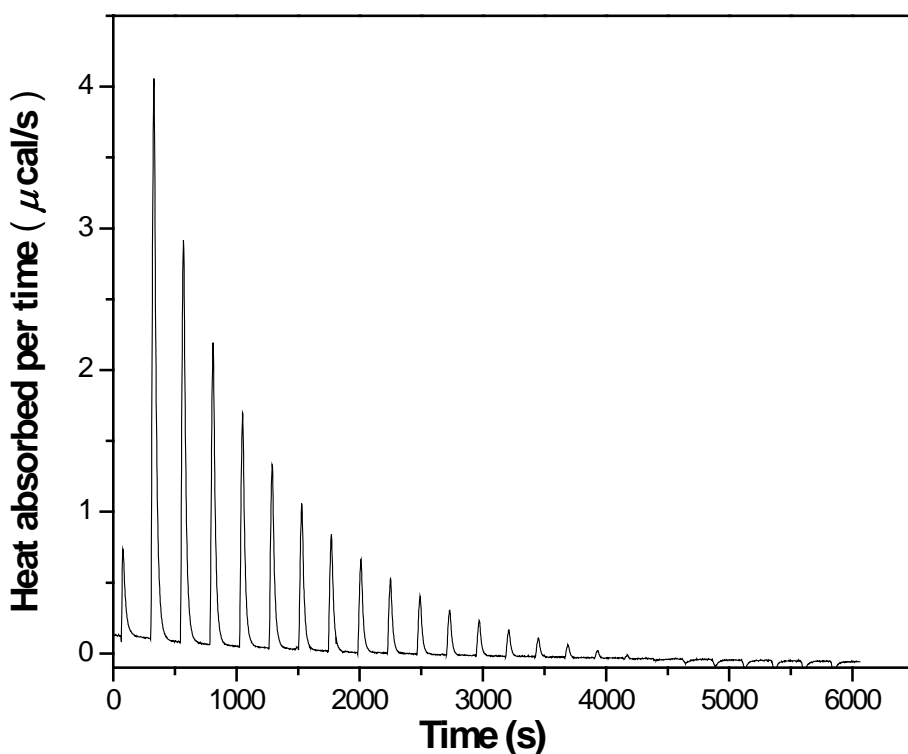
Figure 1.7   ITC data for a preliminary injection of 2 µl and 24 injections of 10 µl of POPC:water dispersion into 1.34 ml of octanol:water suspension, with concentrations of 20 mM and 4 mM, respectively. The temperature of the experiment was 25°C.

1.3.2 The ITC Fitting Model

In this section, we will present a model to show how we determine the partition coefficient from the heat values. To achieve this, we will first find the change of enthalpy in terms of the number of molecules of octanol in the two different phases and the heat of dilution. The expression for the heat per mole of lipid injected is then calculated. Next, we find the relevance of this expression to the partition coefficient based on the definition of partition coefficient for this experimental method. Finally, the heat per mole of lipid injected is expressed in terms of three unknown parameters, which will be determined from fitting to the experimental data, and several experimental constants that are determined from the sample preparation conditions.

1.3.2.1 Change of Enthalpy

After each injection, some of the octanol molecules bind to the lipid bilayers while others remain free in water. If the initial number of moles of solute (1-octanol) bound to the lipid bilayers before injection is N_{sb} and the initial number of moles that are free in water before injection is N_{sw}, the enthalpy of the system can be written as

$$H^0 = N_{sb} h_b + N_{sw} h_w , \qquad (1.1)$$

where h_b and h_w are the enthalpy per mole of solute (1-octanol) in bilayer and in water, respectively. After an injection of a volume ΔV_i of lipid suspension, the number of moles of 1-octanol in bilayer and in water will change to N'_{sb}

and N'_{sw}, respectively. Therefore, the corresponding enthalpy of the system after injection is

$$H' = N'_{sb} h_b + N'_{sw} h_w + \Delta H_{dil} , \qquad (1.2)$$

where ΔH_{dil} is the change of enthalpy due to the dilution by volume ΔV_i. As a result, the change of enthalpy upon injection of the lipid dispersion into the ITC measuring cell containing the 1-octanol dispersion can be written as

$$\Delta H = H' - H^0 = (N'_{sb} - N_{sb}) h_b + (N'_{sw} - N_{sw}) h_w + \Delta H_{dil} \qquad (1.3)$$

$$= \Delta N_{sb} h_b + \Delta N_{sw} h_w + \Delta H_{dil} .$$

It should be noted that the total number of 1-octanol molecules in the cell is conserved, thus $\Delta N_{sb} = -\Delta N_{sw}$. Therefore Eq. 1.3 can be rewritten as

$$\Delta H = \Delta N_{sb} (h_b - h_w) + \Delta H_{dil} . \qquad (1.4)$$

1.3.2.2 Heat per Mole of Lipid Injected

If the molar concentration of the lipid dispersion used is n_l, then the number of moles of lipid injected or the change in the total number of moles of lipid in the ITC cell ΔN_l is

$$\Delta N_l = n_l \Delta V_i .$$

Therefore, the heat released or absorbed per mole of lipid injected, q can be written as

$$q = \frac{\Delta H}{\Delta N_l} = \frac{\Delta N_{sb} (h_b - h_w) + \Delta H_{dil}}{\Delta N_l} = \frac{\Delta N_{sb} (h_b - h_w)}{\Delta N_l} + \Delta h_{dil} , \qquad (1.5)$$

where Δh_{dil} is the heat of dilution per mole of lipid injected. Introducing Δh_{int}, the heat of interaction, the change of enthalpy per mole of 1-octanols from that in water to that in bilayer,

$$\Delta h_{int} = h_b - h_w \,, \tag{1.6}$$

Eq. 1.5 can be written as

$$q = \frac{\Delta N_{sb}}{\Delta N_l} \Delta h_{int} + \Delta h_{dil} \,. \tag{1.7}$$

1.3.2.3 Partition Coefficient and Fitting Model

The partition coefficient is defined as the ratio of the mole fraction of the partitioned molecules to the mole fraction of free/non-partitioned molecules. Therefore, in this experiment, the partition coefficient of 1-octanol molecules into the lipid bilayers is defined as

$$K_p = \frac{X_{sb}}{X_{sw}} \,, \tag{1.8}$$

where X_{sb} and X_{sw} are the mole fractions of 1-octanol molecules in the lipid bilayer and in water, respectively. We can write X_{sb} in terms of molar concentration of 1-octanol in bilayer N_{sb},

$$X_{sb} = \frac{N_{sb}}{N_{sb} + N_l} \,, \tag{1.9}$$

where N_l is the total number of moles of lipid injected. Also we can write X_{sw} in terms of molar concentration of 1-octanol in water N_{sw},

$$X_{sw} = \frac{N_{sw}}{N_{sw} + N_w} \,, \tag{1.10}$$

where N_w is the total number of moles of water in the ITC cell. The total number of moles of water in the ITC cell after injection number i is equal to the initial number of moles of water in the cell before injections (in the original octanol:water suspension) plus the moles added to the cell due to the injections:

$$N_w = N_{wo} + n_w V_i,$$
(1.11)

with N_{wo} and n_w being initial number of moles of water in the cell and the molar concentration of water in the lipid suspension, respectively, and V_i being total volume injected into the ITC cell after injection number i. From Eqs. 1.8, 1.9 and 1.10 we can rewrite the partition coefficient in terms of the corresponding mole concentrations of 1-octanol in water and in bilayer and the total numbers of moles of lipid and water,

$$K_p = \left(\frac{N_{sb}}{N_{sb} + N_l}\right)\Big/\left(\frac{N_{sw}}{N_{sw} + N_w}\right).$$
(1.12)

Using the total number of moles of 1-octanol,

$$N_s = N_{sb} + N_{sw},$$
(1.13)

we can substitute N_{sw} in Eq. 1.12 with $N_s - N_{sb}$, and write

$$K_p = \frac{N_{sb}(N_s - N_{sb} + N_l)}{(N_s - N_{sb})(N_{sb} + N_l)}.$$
(1.14)

Solving Eq. 1.14 for N_{sb}, we find

(1.15)

N_{sb}

$$= \frac{K_p(N_s - N_l) - N_w - N_s + \sqrt{K_p^2(N_s^2 + 2N_lN_s) - N_s^2(2K_p - 1) + 2N_s(N_w - K_pN_w - K_pN_l) + (K_pN_l) + (K_pN_l + N_w)^2}}{2(K_p - 1)}.$$

Using the approximation $\frac{\Delta N_{sb}}{\Delta N_l} \cong \frac{\partial N_{sb}}{\partial N_l}$, and calculating the partial derivative of

N_{sb} in Eq. 1.15 with respect to N_l, we find

$$\frac{\Delta N_{sb}}{\Delta N_l} \cong \tag{1.16}$$

$$-\frac{K_p}{2(K_p-1)} + \frac{2K_p^2(N_s+N_l)+2K_p(N_w-N_s)}{4(K_p-1)\sqrt{K_p^2(N_s^2+2N_lN_s)-N_s^2(2N_s(N_w-K_pN_w-K_pN_l)+(K_pN_l+N_w)^2}} \;.$$

Equation 1.16 shows that $\frac{\Delta N_{sb}}{\Delta N_l}$ is a function of four parameters: $N_s, N_l, N_w,$

and K_p. N_s, the initial number of moles of octanol, is constant during the

experiment. N_l, the total number of moles of lipid in the cell, is the independent

parameter which varies during the experiment as the number of injections of the

lipid sample increases. According to Eq. 1.11, N_w depends on two constants, N_{wo}

and n_w, and a changing parameter, V_i, which can be written as

$$V_i = \frac{N_l}{n_l}. \tag{1.17}$$

Thus, N_w can be written in terms of three constants and the independent

parameter of the fitting equation, N_l. Finally, K_p, the partition coefficient of 1-

octanol into lipid bilayers, is the unknown parameter which is being derived from

fitting Eq. 1.7, with substitution of $\frac{\Delta N_{sb}}{\Delta N_l}$ from Eq. 1.16, to the experimental data.

It is explained in Ch. 3 that Eq. 1.7 and 1.16 together are used for fitting

the data of the heat released or absorbed per mole of lipids, and finding the

partition coefficient, the heat of interaction and the heat of dilution parameters.

CHAPTER 2:
MATERIALS, EXPERIMENTS AND METHODS

This chapter includes a review of the materials, methods and experiments used in this study. The first section explains the procedure of mixing POPC and cholesterol, and also the preparation of the vesicle suspensions for ITC experiments. A detailed description of ITC, the main experiment of this study, is the subject of Sec. 2.2; this description includes the apparatus, setups, and experimental procedures.

2.1   Lipid Mixture and Vesicle Preparation

2.1.1   Materials

The lipids used in this study are 1-palmitoyl-2-oleoyl-*sn*-glycero-3-phosphocholine (POPC) and cholesterol. Both were purchased in powder form from Avanti Polar Lipids Inc., Alabaster AL. For these experiments, POPC is used both in pure state and mixed with cholesterol at different molar ratios. A full description of the structure and properties of POPC and cholesterol can be found in Ch. 1.

2.1.2   Lipid Mixture Preparation

To guarantee a uniform, homogenous and well-mixed mixture of POPC and cholesterol, these materials were lyophilized first. Lyophilization or freeze-drying is a dehydration process where the solvent molecules in the

solution/dispersion are eliminated by evaporation from the solid phase under reduced pressure and the solute molecules, which are not vaporizable, are left behind. While the solvent molecules sublimate under a low pressure, the solute lipid molecules cannot rearrange since they remain in the solid phase, according to their phase diagram at that low pressure. Therefore, when the lyophilized mixture is hydrated the molecules of POPC, or any other similar lipid, and cholesterol will be mixed uniformly [29]. The solvent used in this method is usually a volatile liquid that can dissolve the solute completely. A 4:1 benzene:methanol mixture was used as the solvent in this study. The calculated portions for the desired molar ratios of POPC and cholesterol were first weighed in a scintillation vial, and then were dissolved in 1-2 ml of the solvent mixture. The mixture was then frozen by inserting the vial in liquid nitrogen. The vial was placed inside the lyophilizer, which pumped off the vapour of the solvent for 6-7 hours in a vacuum below 8 mtorr.

To prepare lipid vesicles, the lyophilized lipid mixture was dispersed in filtered deionised water from a Milli-Q Plus filtration system (Millipore, Bedford MA) inside a cryogenic vial (Nalge Company, Rochester NY). The dispersion was taken through a freeze-thaw-vortex sequence five times. This process consists of freezing the sample by submerging the vial in liquid nitrogen for 5 minutes, then thawing it by immersing in the water bath (Branson 3200) at 50°C for 5 minutes and vortexing it for the same duration. This technique helps to disperse the lipids in water by breaking the aggregates and produces large multilamellar liposomes.

The multilamellar liposomes should then be extruded to form the unilamellar vesicles to be used in the ITC experiments.

2.1.3 Vesicle Preparation for ITC

After the freeze-thaw-vortex process, the sample was diluted to 20 mM, which has been found to be the ideal concentration for ITC measurement of these lipids based on the work of Dr. Philip J. Patty (unpublished). This concentration yields heat changes that have an appropriate magnitude for detection and analysis. A diagram of the extruder (Lipex Biomembranes, Vancouver BC) is shown in Fig. 2.1. The dispersion was transferred to the chamber of the extruder with a syringe. For all of the extrusions, high-purity nitrogen gas was used to apply the pressure at the top of the sample chamber through the high-pressure gas inlet and valve. The range of the pressure used in the experiments was 20 to 200 psi, and a regulator was used with a maximum pressure of 400 psi. The applied pressure pushes the dispersion containing vesicles through the cylindrical pores of the filters. A tube was connected to the outlet at the bottom of the extruder, which carried the extruded sample to a test tube. All extrusions were maintained at room temperature.

As the first step, a 4-5 ml aliquot of the dispersion was extruded through two stacked polycarbonate membrane filters (Whatman International Ltd.), with a nominal pore diameter of 400 nm held in the base of the extruder. This step is called pre-extrusion and requires a pressure of 20-30 psi. It helps change the multilamellar vesicles into unilamellar ones and facilitates further extrusions with 100 nm filters at this rather high concentration of lipids.
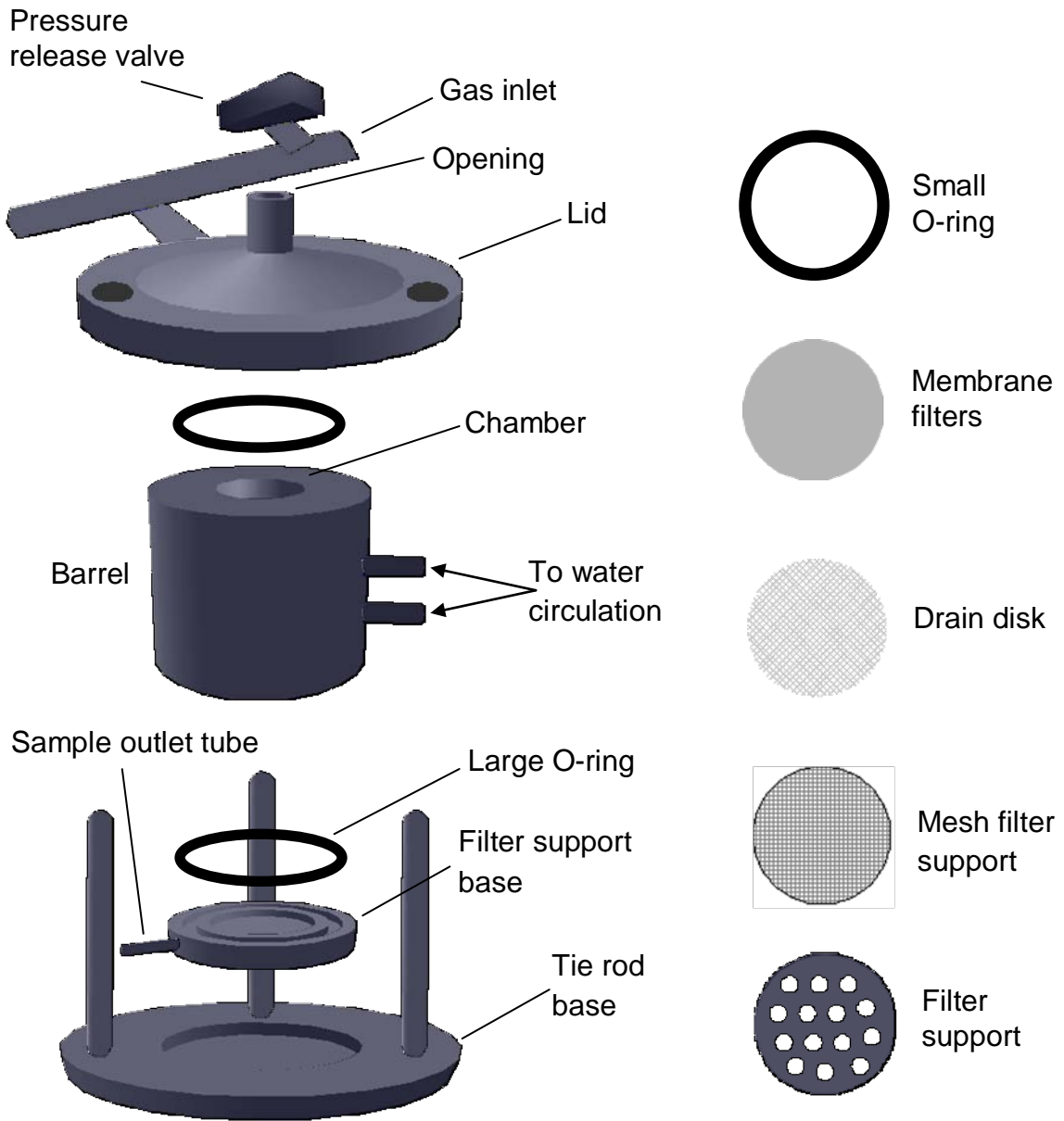
Figure 2.1 **A schematic diagram of the extruder. The filter support base sits on top of the tie rod base. A stainless steel filter support, a metal mesh filter support, a drain disk, two stacked membrane filters, and finally a small O-ring sit on top of each other, in the mentioned order; all fit into the central cavity of the filter support base . The barrel is placed over the base, and the lid is threaded through the tie rods, put on top of the barrel and tightened firmly. Two large O-rings are used on the filter support base and barrel to seal the unit. The sample is injected into the chamber inside the barrel through the opening of the lid, and the cap of the lid (not shown) is tightly closed to seal the opening of the lid. A plastic tube (not shown) is connected to the sample outlet tube of the filter support base. Water at the desired temperature is circulated through two plastic tubes connected to the barrel to maintain the barrel and the sample at the required temperature.**

After pre-extrusion, another step was taken in order to better facilitate the final extrusion with 100 nm membrane filters, which is the desired size for the vesicles. The sample was next extruded five times with two stacked 200 nm filters at a pressure starting from 70 psi and up to 120 psi for the last drops for each extrusion. Between extrusions, the dispersion was transferred with a syringe from the test tube containing the extruded sample back to the extruder for the next extrusion. Finally, the dispersion was extruded through two stacked 100 nm filters at least another five times, at a pressure starting from 110 psi up to 170 psi. This provided a total number of extrusions of at least 10.

The samples were held in a capped test tube, sealed with Parafilm (American Can Co., Greenwich CT), and stored in the refrigerator to be used the following day.

2.2 ITC Measurements

The ITC measurements were performed at UBC (University of British Columbia, Vancouver BC) Michael Smith Laboratories, under the supervision of Dr. Louise Creagh. The MCS-ITC equipment (MicroCal Inc., Northampton MA), Micro Calorimetry System with Isothermal Titration Calorimetric unit, was located in the BioThermodynamics lab inside the Michael Smith Laboratories building.

In this section, the ITC instrument and the experimental procedures will be explained. Most of the information about the instrument operation, setup and settings and the relevant figures are adapted from MicroCal manual for MCS-ITC and MCS-DSC instruments [30].

2.2.1 MCS-ITC Instrument

The MCS system consists of several different parts: a Controller Unit, a Calorimetric Unit, a refrigerated water bath, a host computer, and associated accessories. The Calorimetric Unit is the ITC unit. All operations of the Calorimetric Unit are supervised directly by the Controller Unit, which communicates with the host computer. The host computer serves as the user interface for sending the commands to initiate the experiments and for displaying the generated data.

The ITC unit directly measures the heat generated or absorbed as a result of injecting precise amounts of one reactant into a solution of the other. A specially equipped syringe is used to inject the sample. The injection syringe has a spiral tip and spins with a user-selected speed which facilitates the subsequent mixing. The default spinning rate of the syringe was selected to be 400 rpm.

There are two cells in the ITC instrument: the sample or measuring cell and the reference cell. Both cells can be reached from the top of the unit for filling and cleaning. The sample cell has a wider opening than the reference cell, providing better accessibility of the sample cell and also protection of the reference cell from pollution by the sample or any cleaning materials.

The sample and reference cells are both coin-shaped and identical, and are enclosed in an adiabatic jacket, as shown in Fig. 2.2. Both cells have access stems of identical shape and length, extending from the cells to the top exterior of the instrument. The disks and stems of both cells have the same volume and are completely filled with equal amount of liquid, approximately 1.7 ml. The sample
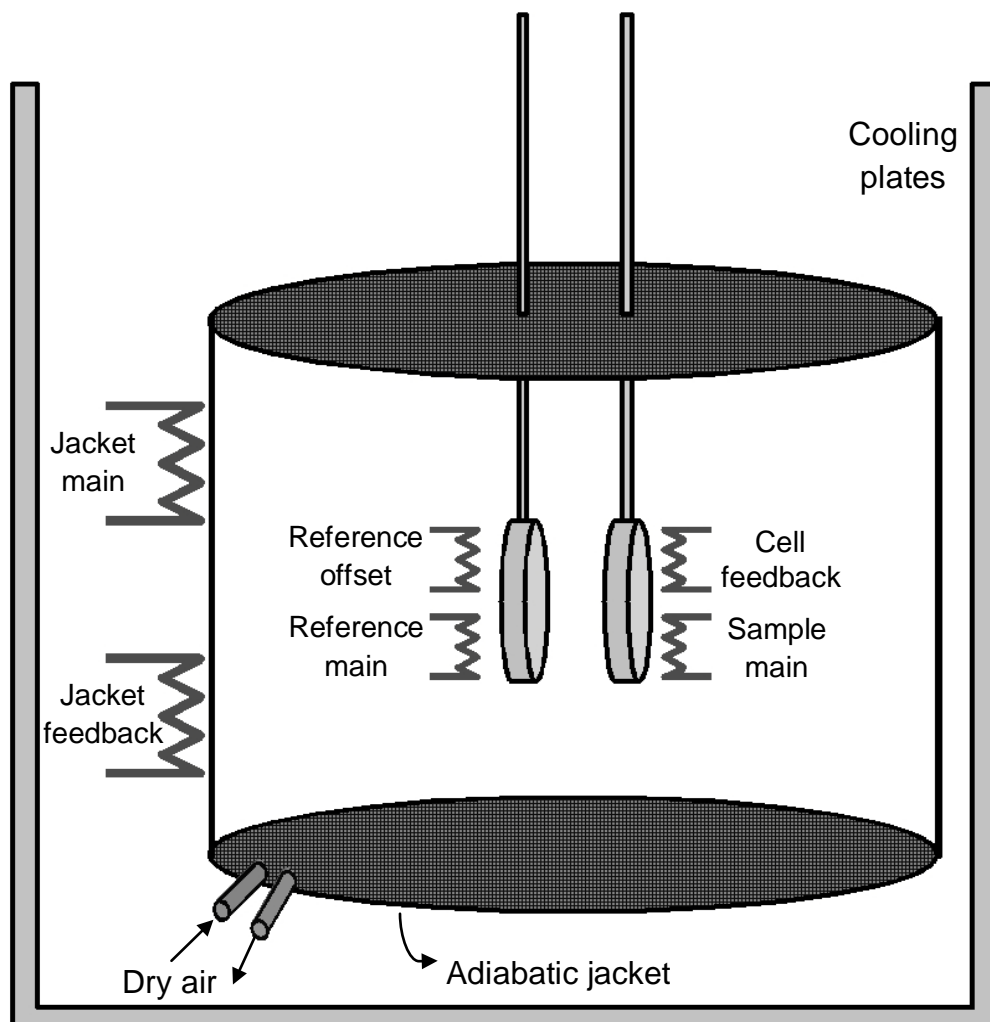
Figure 2.2 **A schematic diagram of the ITC unit, adapted from [30]. The sample and reference cells are inside an adiabatic jacket, which provides an adiabatic environment for the experiment. The jacket is ventilated by circulating dry air through it. The outer surfaces of the cells are coated with resistive heating elements and are heated by different heaters, as shown by resistor symbols.**

cell is filled with a dilute solution of a substance in a solvent, normally water, and the reference cell is filled the same solvent.

The outer surfaces of the cells are coated with resistive heating elements. During an experiment both cells are heated by a constant power to their main heaters, as labeled by sample main and reference main in Fig. 2.2. A second

heater, the reference offset, heats the reference cell by a small additional constant power. The temperature difference between the two cells is measured and the cell feedback system increases or decreases the applied power through the cell feedback heater in proportion to the temperature difference in order to keep it close to zero. The signal proportional to that feedback power is called the CFB and is reported in units of µcal/sec. The time-varying CFB data together with the instrument temperature constitute the experiment's raw data. If heat is evolved or absorbed through the chemical reaction after the injection, the appropriate CFB is applied by the feedback system; i.e. if heat is evolved, the CFB is decreased and there is a peak downward in the CFB power, and vice versa. Therefore since the CFB has units of power, the time integral of the area under a downward or an upward peak yields a direct measurement of the heat released or absorbed, respectively.

There are also two heaters connected to the jacket. The jacket main heater applies a constant power to the jacket. The jacket feedback system constantly monitors the temperature difference between the cells and the jacket and the power applied to the jacket resistive heater is proportionally increased or reduced in order to keep this difference close to zero. The temperature difference, ΔT, is presented as the secondary data.

2.2.2 Experiment Setup

Prior to every ITC run, all of the syringes and the ITC cell were prepared to ensure that they were clean and dry. There were five different syringes associated with the sample setup including the injection syringe, which is filled

with sample and will be discussed in detail, two 2.5 mL Hamilton syringes, which are used to fill and rinse the cell, and two plastic syringes of different sizes, which are used for filling and rinsing the injection syringe.

2.2.2.1   Sample Preparation

As the first step in sample preparation, both cell and syringe samples were degassed in order to guarantee bubble-free loading of the samples. The degasser that was used consisted of a diaphragm pump and a plastic vacuum chamber placed on top of a magnetic stirrer. To avoid contaminating the samples and losing some octanol that may stick to the magnetic stir bar, the degassing was done without stirring, and therefore for a longer time. Every sample was degassed for two periods of 5 minutes.

2.2.2.2   Filling the Injection Syringe

The injection syringe, illustrated in Fig. 2.3, consists of a plunger, a capillary, an input port, and a needle consisting of a spiral lower part and a stirring paddle. The injection syringe was mounted inside a plastic holder, as shown in Fig. 2.3, during all procedures.

The syringe capillary should be completely dry before filling; therefore there is a risk of entrapping air bubbles while filling the syringe. In order to prevent this, a special filling procedure, illustrated in Fig. 2.4, was followed. While the syringe was seated on the Plexiglas stand, its plunger was raised up to the high edge of the input port. The syringe tip was submerged in a small culture tube that was filled with the lipid vesicle solution. A second syringe, a plastic

filling syringe, was connected to the input port with a thin flexible plastic tube. This allowed for the suction of the liquid into the injection syringe, and the elimination of all the air between the plunger and the liquid. Once the sample started to exit the port, the plunger was pushed down below the port. The plastic tube was then removed from the input port.
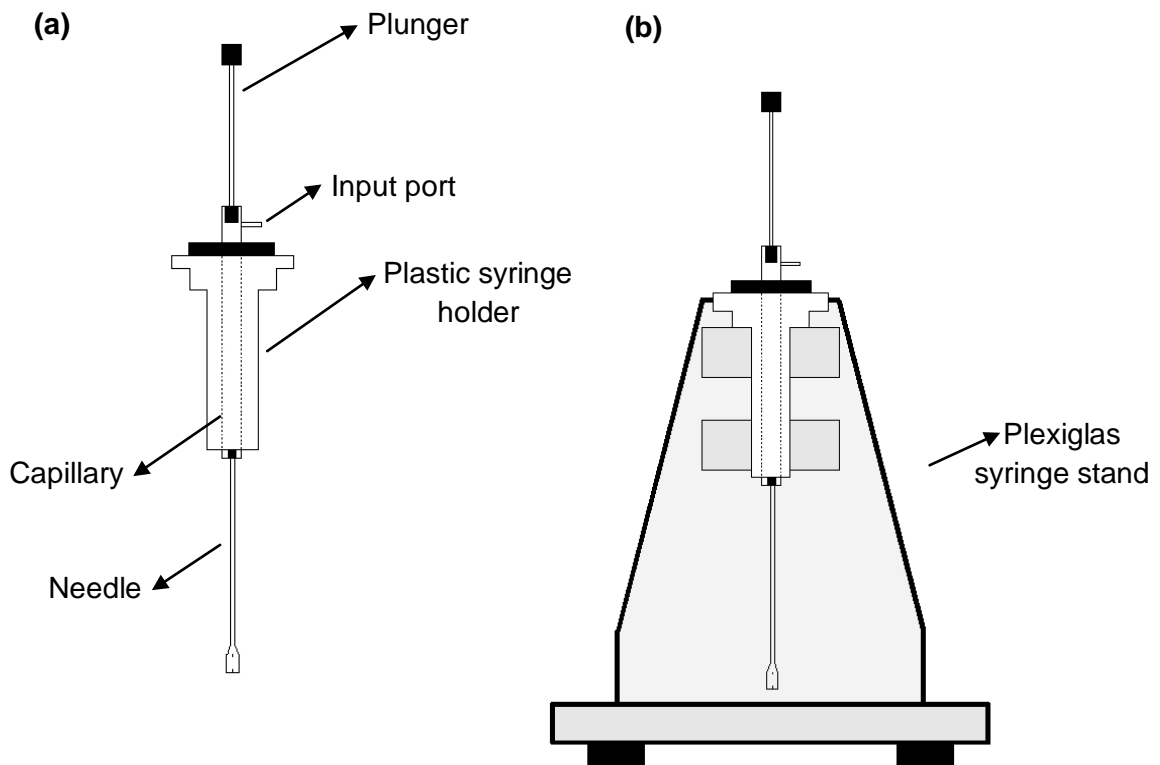
Figure 2.3   (a) The injection syringe inside the plastic holder. The syringe should be inside the syringe holder during all procedures. (b) The injection syringe seated on the Plexiglas syringe stand. The injection syringe was seated on the stand during the filling and cleaning procedures of the syringe. (Adapted from [30])

In order to ensure that any small bubbles formed in loading were expelled out of the long needle, the plunger was first pushed down sharply with the paddle still immersed in the sample and then was pulled up so that the solution was

drawn slowly back up. This procedure was repeated four-five times. There are two tiny apertures, one at the bottom of the paddle and a second about 1 cm above the bottom. It should be noted that the liquid transfer into and out of the syringe occurs through the higher aperture and that the liquid level should always be higher than this aperture.
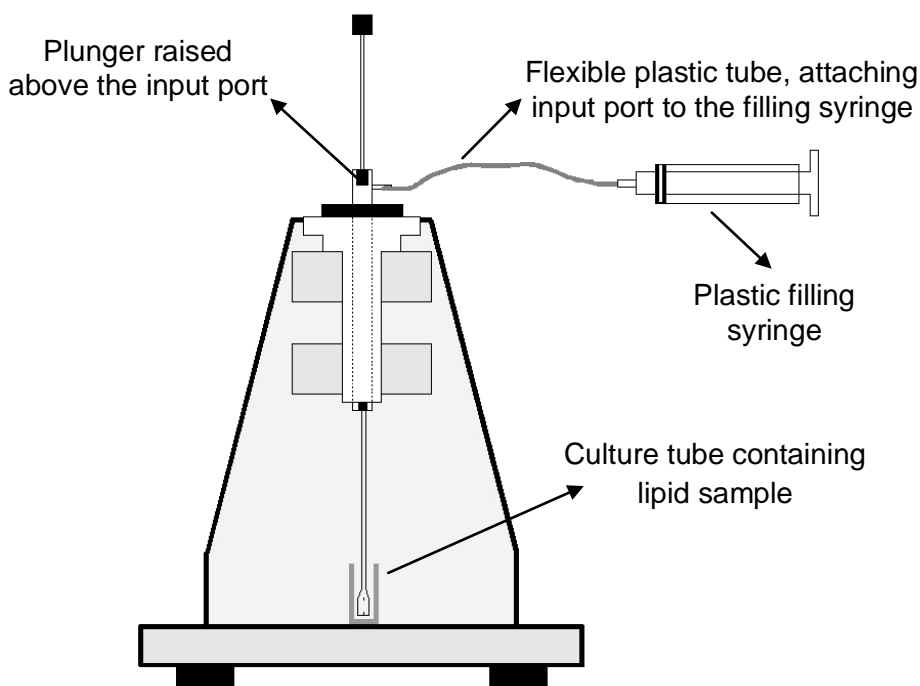
Figure 2.4   The filling configuration of the injection syringe using a plastic filling syringe, a flexible plastic tube and a culture tube. The liquid transfer into and out of the injection syringe occur through a tiny aperture above the bottom of the paddle. (Adapted from [30])

After filling, the tip of the syringe was first rinsed lightly with purified water from a rinsing bottle, and then was dried very carefully with a Kimwipe tissue and seated back onto the syringe stand. While drying the syringe, attention was required to prevent touching the two apertures on the stirring paddle. Also it was very important not to flex the syringe because the syringe was filled with the

titrant which could be displaced, resulting in an error in the injection volume of the first or subsequent injections. Then the syringe was left on the syringe stand to completely dry externally, during the cell loading procedure.

2.2.2.3 Loading the ITC Cell and Final Setup

The cell was loaded and cleaned with two long-needled 2.5 mL Hamilton syringes, here called the cleaning and loading syringes. The loading syringe was used to transfer the octanol:water suspension and the cleaning syringe was used to remove the water from the cell and also to perform further cleaning, as described in the next section. Since the cell should never be left empty, it was always loaded with water between experiments. At the start of an experiment, the water was removed and then the cell was loaded with the solution and unloaded five times, so that the concentration of the solution inside the cell became unaffected by the remaining water. The cell was filled from bottom to top each time. The top of the access tubes are visible at the bottom of the injection system. The sample cell is in the center and the reference cell is on the left as one faces the front of the unit. The cell was loaded slowly until the liquid slightly overflowed the access tube. Then the liquid was removed from the cell using the syringe and was disposed of in a disposal container beside the instrument. The syringe was refilled and this procedure was repeated five times.

For the fifth loading procedure, there was an extra step taken to expel any possible small bubbles left near the top of the cell. When the cell was almost completely filled, the last 1 mL was injected with an abrupt spurt in order to dislodge any bubbles. The needle of the syringe was then agitated and tapped

on the bottom of the cell in order to dislodge any trapped bubbles in the cell. Then another 1 mL volume was removed using the loading syringe and this procedure was repeated, for a total of five times. After the last repetition, the syringe was removed from the cell, and any excess liquid around the access tube was removed using the loading syringe.

After the cell had been loaded with the octanol:water suspension, the injection syringe was removed from the syringe stand and was inserted carefully inside the injection system. Again this was done very carefully in order to avoid any displacement of the titrant inside the loaded syringe. The needle was placed carefully through the cell tube, and when the syringe holder was seated on top of the injection system properly, a final push with a click fixed it in its place.

2.2.2.4 Cleaning

After each experiment, some cleaning steps were taken using the cleaning syringe. Cleaning the ITC sample cell consists of three steps. After discarding the remnants inside the cell, it was rinsed with pure water 10 times. During rinsing, the cell was filled with a sufficient amount of liquid and then emptied. It was then rinsed with methanol or ethanol 5 times. Finally, it was washed with more water another 10 times. The cell was filled with water if it was the final experiment of the day. After filling the cell with water, the excess water around the access tube of the cell was removed.

In order to clean the injection syringe, the excess lipid solution was discharged by pushing the syringe plunger to the end carefully. The inside and outside of the syringe and its plunger were then rinsed well with lots of pure

water. The syringe was then put pack together and was seated on the syringe stand. A mixture of a surfactant at 5% concentration, provided in the lab, was then used for rinsing the syringe. The setup shown in Fig. 2.4 was repeated with a larger plastic syringe designated for cleaning, and also a larger plastic tube instead of the glass culture tube. The syringe was rinsed 5 times with the soap solution with the same procedure explained before for filling the syringe. Then it was rinsed with pure water using the same method 5 times. Finally, the syringe was dried by flowing nitrogen gas through its input port for 2 minutes with its plunger in place and a further 10 minutes without its plunger.

2.2.3 Running the Experiment

All ITC measurements were carried out at a temperature of 45°C. There is a possibility of baseline degradation when operating far above room temperature. Therefore, the thermostat temperature was set to 45°C one day ahead of the experiment day, and was allowed to equilibrate overnight. For experiment execution and settings, MCS Observer software was used as the user interface to the MCS Control Unit. This software collects data from and issues command sequences to the MCS Control Unit. It also communicates with MicroCal's data plotting and analysis software, Origin (Origin Lab, Northampton MA). Data that is collected at the host computer is sent to Origin and is plotted there. Origin is also used for the data analysis of the MCS collected data, which will be fully discussed in Ch. 3.

By running the MCS Observer software on the host computer, the MCS software operating system (MCS OS) communicates with the Control Unit. The

MCS OS starts operating the MCS Control Unit and the MCS Observer begins several initialization procedures. The Observer's main window will then appear, as in Fig 2.5, allowing the user to acquire the instrument control menus and displaying live data of the cell unit. Below is the list of explanations of the associated MCS data channels. The Observer window normally displays the following data:
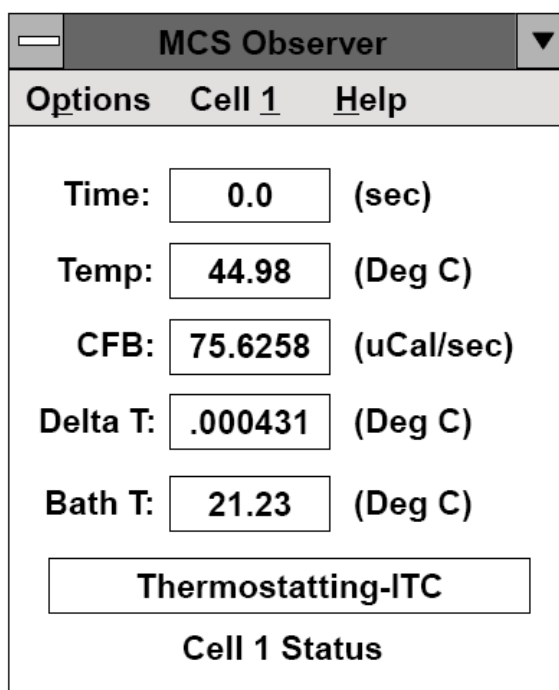
Figure 2.5   MCS Observer window as it appears on the computer screen, adapted from [30].

Time: The current time in seconds. The time data starts once the experiment is executed and is reset to zero when the equilibration starts and when it is complete and the actual run begins.

Temp (Temperature): The current temperature of the jacket.

CFB (Cell Feedback): The data of the applied feedback power to the sample cell.

Delta T (ΔT): The temperature difference between the jacket and the sample and reference cells. Positive ΔT means cells are warmer than the jacket.

Bath T (Bath Temperature): The current temperature of the external water bath in degrees Centigrade. It should be noted that this is not the bath's target temperature and that the current target temperature of the cells may be changed as will be described later.

Cell Status: The current state of the cell. The Cell Status Box updates the status of several pre-run states as the run proceeds.

An Origin window also appears with the Observer's window which will show the pre-run live plots. During the run, plots of CFB, Delta T and temperature (Temp) are displayed with different colours as a function of time on the Origin window.

The experimental temperature was set using the Set Thermostat Temp option from the Cell 1 drop-down menu of the MSC Observer window, as shown in Fig. 2.6. As mentioned before, this was usually done one day in advance of the experiment, unless two measurements with different temperatures were made on the same day, which needed some time for the instrument to find its equilibrium.

The MCS Observer also allows the user to specify the settings for a run using the Cell 1 drop-down menu, as pictured in Fig. 2.6, and selecting the first option, ITC Setup. In the ITC Injection Setup window (not shown), three sets of

parameters must be specified for each titration experiment. The injection parameters and their values are listed in Table 2.1. The filter parameters were left at their default values, which are listed in Table 2.2. The concentration parameters include "In Syringe" and "In Cell" concentrations in mM that were set according to the samples. The cell was always filled with octanol:water dispersion at 4 mM and thus its concentration was always set to 4 mM. The syringe was filled with the lipid dispersion at nominal concentration of 20 mM; however the exact concentrations fluctuated around this value according to different sample preparations.
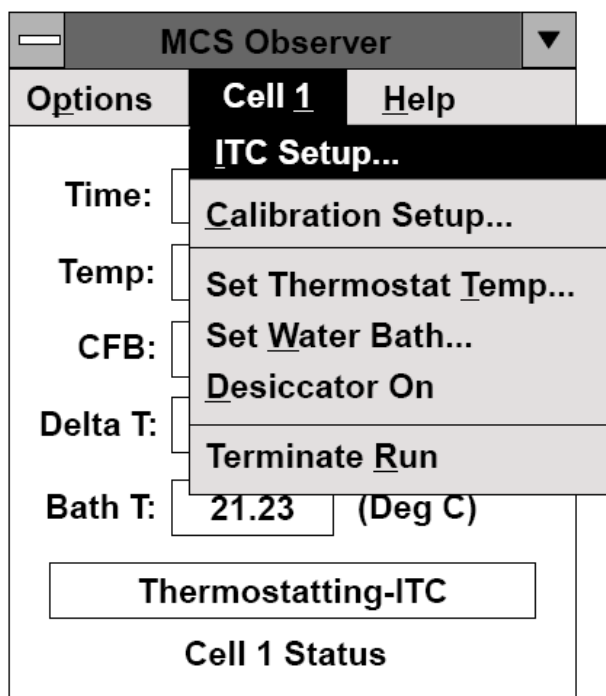
Figure 2.6   The ITC Cell 1 drop-down menu, adapted from [30].

Injection Parameter	Value
Number of Injections	25
Experimental Temp.	45 Deg. C
Initial Delay	60 sec
Volume	10 µl *
Injection Duration	25 sec
Time between Injections	240 sec
Reference Offset	5% Ref. Power

Table 2.1   The Injection parameters in the ITC Injection Setup window and their values as it was set in every ITC experiment. *The volume of all injections was 10 µl, except for the first injection that was set to 2 µl,

Filter Parameters	Value
t 1	2 sec
t 2	2 sec
t Switch	240

Table 2.2   The filter parameters in the ITC Injection Setup window and their default values.

The volume of the first injection was changed to 2 µl using the Unique Injection option in the ITC Setup window. The first injection volume may have some inaccuracy due to the filling and mounting of the injection syringe. Therefore, a preliminary injection of a small volume was made and its corresponding heat signal was not considered for data analysis.

The experiment was started by selecting the Execute Run button in the ITC Setup window. By doing so, a small window appeared on top of the setup

window showing the initiation of the start of the ITC experiment and the transmission of the run parameters to the MCS Control Unit.

After all injections were completed, the data file of the run was stored as an Origin file that could be exported for further analysis. The instrument's injection unit automatically returned to its initial position making the injection syringe accessible for removal. The injection syringe and the ITC cells were then ready to be cleaned as described in Sec. 2.2.2.4.

CHAPTER 3: RESULTS

This chapter contains the isothermal titration calorimetry results, including two different sets of measurements at different molar ratios of POPC and cholesterol. The ITC raw data was analysed and the model function, described in Ch. 1, was fit to the data. One of the three fitting parameters is the partition coefficient of 1-octanol molecules into lipid membranes. The partition coefficients, heats of interaction and heats of dilution were plotted as a function of cholesterol content. The results of partition coefficient graphs from two different data sets are consistent; they show an increasing trend of partition coefficient with increasing cholesterol content.

3.1 Typical ITC Data, Analysis and Fitting

In this section, the ITC data for the pure POPC sample is presented as a typical result. Then the detailed analysis and fitting procedure are demonstrated, which are extendable to the next sections.

As explained in the previous chapters, the ITC experiments included 25 injections of the lipid dispersion from the injection syringe into the octanol-water suspension inside the ITC cell. Figure 3.1 shows the graph of the raw ITC CFB data for 25 consecutive injections of a dispersion of POPC vesicles in water at a concentration of 19.1 mM into a 4.0 mM octanol-water suspension at T=45°C. The volume of the first injection was chosen to be small, 2.00 μl, for the reasons

explained before and it is excluded from the analysis. Therefore, the peak produced by this injection is smaller compared to the next injection. The volume of the rest of 24 injections was 10.0 µl and the injections were separated by 4-minute (240-second) time intervals.
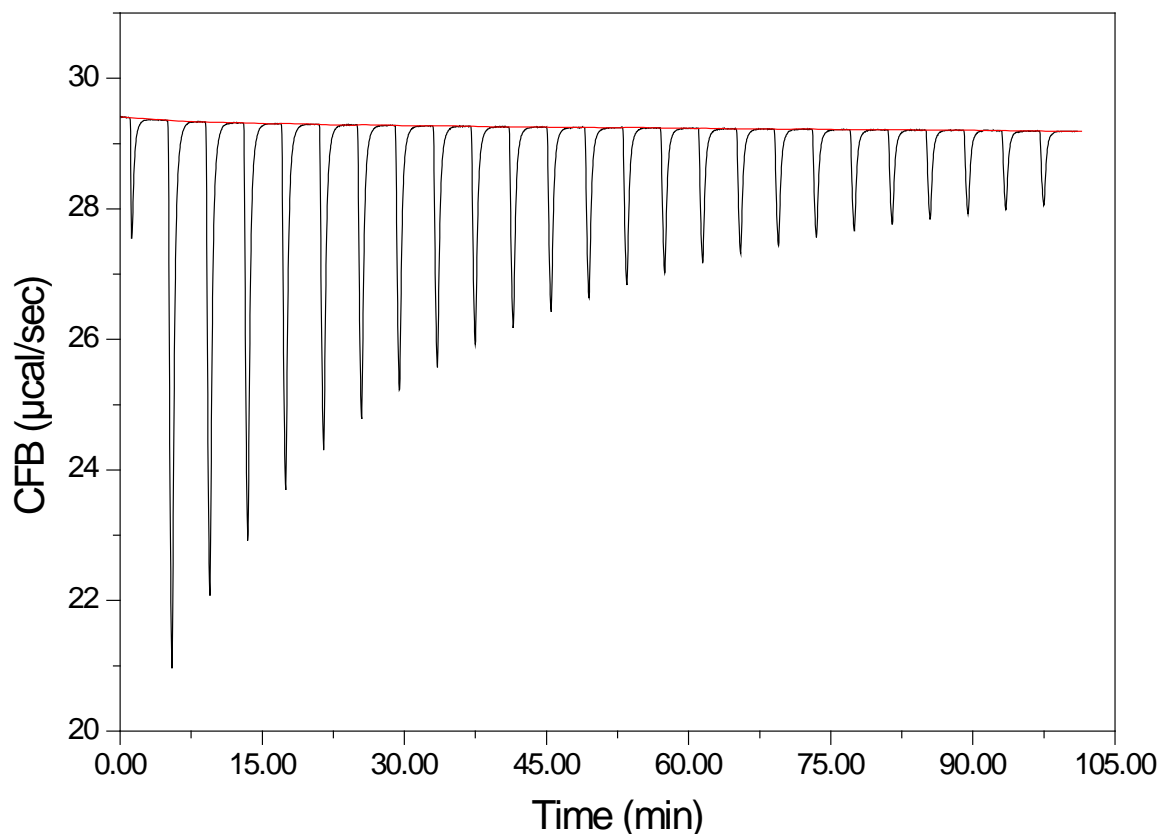
Figure 3.1 ITC CFB results for 25 injections of POPC vesicles into an octanol:water suspension. The concentrations of lipids and octanol in water were 19.1 mM and 4.0 mM, respectively. The measurements were conducted at T=45.4°C. The volume of the first injection was set to 2.00 µl, and the volume of the subsequent injections was 10.0 µl.

An injection that causes an exothermic reaction results in the chemical evolution of heat within the sample cell and produces a downward peak in the cell feedback power since the heat evolved chemically provides heat that the cell

41

feedback is no longer required to provide. The opposite is true for endothermic reactions where heat is removed from the system. Therefore, the data in Fig. 3.1 clearly demonstrates that the interaction that occurs after injecting POPC vesicles into the suspension of octanol in water is exothermic and releases heat.

Since the cell feedback has units of power, the time integral of each peak in Fig. 3.1 yields a measurement of the change in thermal energy ΔH as a result of that injection. It is clear that there is a decreasing trend of the heat released in each injection as the number of the injections increases. This is because the number of free octanol molecules in the cell that are available to interact with the injected lipid vesicles decreases after each injection step.

According to our model, the octanol molecules are partitioned into two groups after each injection: some bind to the lipid bilayers and the others remain free in water. The main goal of this study is to measure this partitioning, and to compare the change in the partitioning of octanol molecules into the lipid bilayers at different molar ratios of POPC and cholesterol at the selected experimental temperature of 45°C.

In order to determine the partition coefficient and the heats of interaction and dilution, the ITC data needs to be analysed. The heat per mole values for the corresponding injections were collected from the Origin data file of the ITC run. This file contains the values of the concentration-normalized heat changes for each injection in calories per mole of injectant added. In addition, the total number of moles of lipid injected into the sample cell was calculated for each injection step using the initial concentration of the lipid suspension. Figure 3.2

shows the plot of the heat per mole of injectant q as a function of total number of moles of lipid injected N_l. The negative values of the heat changes confirm that the reactions are exothermic. The absolute values of the heats released decrease with the number of injections. The heat released data seems to approach a saturation in the last injections, which is due to the reduction in the number of free octanol molecules in the sample cell available to interact with the newly injected lipid vesicles. Eventually, after several more injections the heats released or absorbed would be only due to the dilution of the molecules inside the cell. The value of the heat of dilution is derived from the fit.
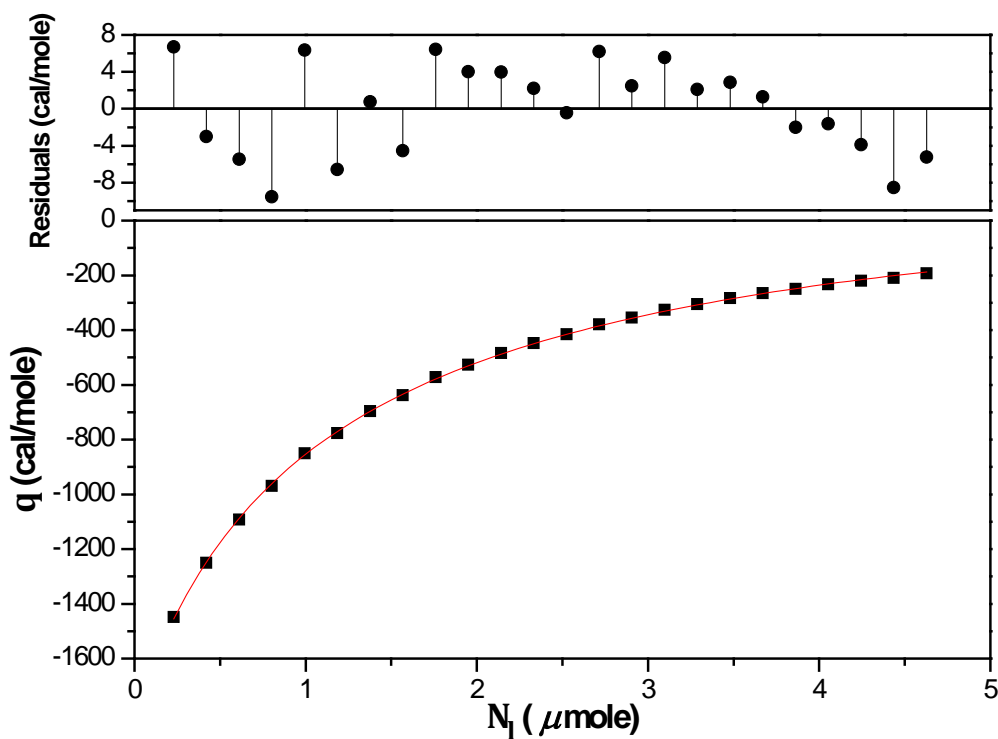
Figure 3.2 **Heat per mole of injectant q as a function of the total mole of lipid injected N_l for 25 injections of POPC vesicles into octanol:water suspension. The concentrations of lipids and octanol in water were 19.1 mM and 4.0 mM, respectively. The heat released in each injection is equal to the area under the corresponding peak in Fig. 3.1. The curve is the fit of Eq. 1.7 to the data, where Eq. 1.16 was used for $\frac{\Delta N_{sb}}{\Delta N_l}$. The values of three parameters, partition coefficient, heat of interaction and heat of dilution, obtained from the fit are shown in Table 3.1.**

The model function presented in Ch. 1 was then fit to the data. The two equations used in the fit are reproduced here for convenience,

$$q = \frac{\Delta N_{sb}}{\Delta N_l} \Delta h_{int} + \Delta h_{dilution} \ , \tag{1.7}$$

where

$$\frac{\Delta N_{sb}}{\Delta N_l} = -\frac{K_p}{2(K_p - 1)} + \frac{2K_p^2(N_s + N_l) + 2K_p(N_w - N_s)}{4(K_p - 1)\sqrt{K_p^2(N_s^2 + 2N_l N_s) - N_s^2(2K_p - 1) + 2N_s(N_w - K_p N_w - K_p N_l) + (K_p N_l + N_w)^2}} \tag{1.16}$$

was used for $\frac{\Delta N_{sb}}{\Delta N_l}$. According to these two equations, q depends on three

parameters: partition coefficient K_p, heat of interaction Δh_{int}, and heat of

dilution Δh_{dil}. The fit of Eq. 1.7 to the data is shown in Fig. 3.2. The plot

demonstrates consistency between the model and the ITC data. The values of

three fitting parameters with the corresponding parameter standard errors are

presented in Table 3.1. Since there is no uncertainty available for the parameters

in the Origin file of the collected ITC data, the fitting is unweighted. The

parameter uncertainties shown in Table 3.1 are the parameter standard errors,

calculated by the Origin software in the fitting process.

K_p(mole frac /mole frac)	Δh_{int} (cal/mole)	Δh_{dil} (cal/mole)
7170 ± 50	-1830 ± 20	146 ± 6

Table 3.1   The fitted values of partition coefficient K_p, heat of interaction Δh_{int}, and heat of dilution Δh_{dil} obtained from fitting Eq. 1.7 to the ITC data for POPC sample.

As the number of injections increases, the heat released decreases and approaches a constant, non-zero value that is the demonstration of the heat of dilution Δh_{dil} in the fitting function. This is where there are no more free octanol molecules left in the sample cell to interact with the injected lipid bilayers; therefore, the heat signals diminish until only heats of dilution are observed. The heat per mole values in Fig. 3.2 appears to trend to a negative value at large N_l, while the heat of dilution determined from the fit, as shown in Table 3.1 is positive. In fact, there is no discrepancy. This is because the number of injections needed for the heat released to reach the saturation value is many more than the number of injections used in these experiments. The high N_l data shown in Fig. 3.2 is very far from the saturation value. To better picture this, the fitting function is extrapolated for 300 injections in Fig. 3.3. It can be observed in Fig. 3.3 that the region covered by the experiment (i=1 to 25) is only the initial portion of the curve and far from the saturation value at the end of the graph. The plot confirms that the heat of dilution is positive and the extremity of the trend is at a positive value.

In the ITC experiments, several lipid samples with varying molar ratios of POPC and cholesterol were studied. By applying the same procedure presented in this section, the partition coefficient, heat of dilution and heat of interaction values were obtained from fitting the model function to the heat data for every lipid sample. The complete data and results of the ITC experiments performed for this study are presented in Section 3.3.
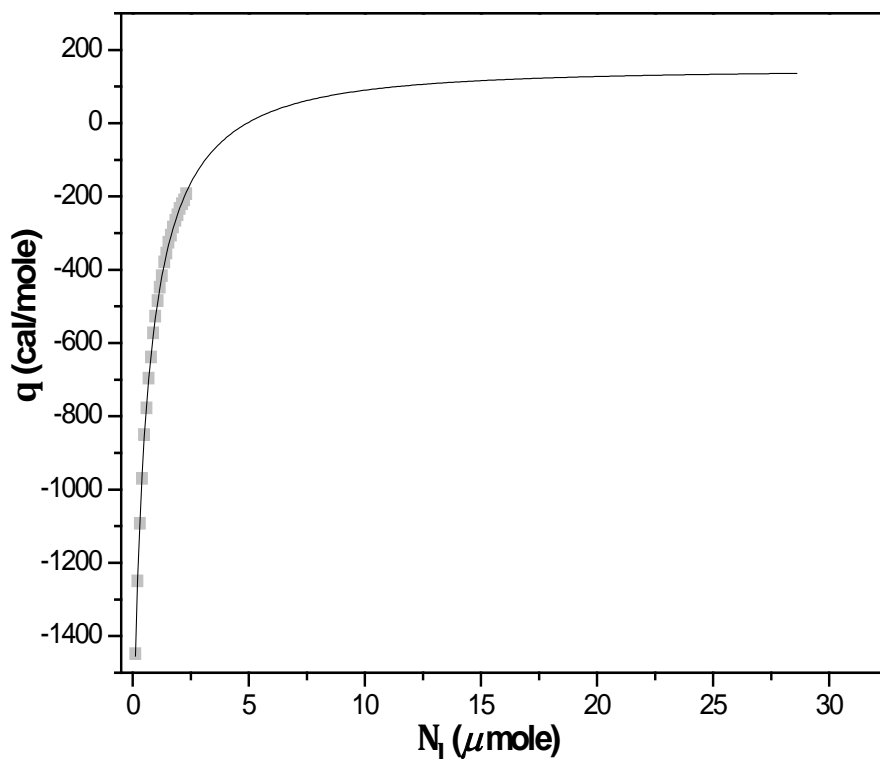
Figure 3.3 **The 25 data points (gray squares) and fitting function of Fig 3.2 as a function of the total mole of lipid injected N_l, extrapolated for 300 injections. The graph trends to a positive value, the heat of dilution, as obtained from the fitting of Eq. 1.7 to the data.**

3.2 Repeatability and Reproducibility of ITC Results

In order to check the reliability of the ITC experiments, two properties of the ITC experiments were probed. The repeatability of the results was tested for one of the prepared samples. In addition, because a problem occurred with the original ITC instrument during the course of experiments and a loaner instrument was provided for the lab during the maintenance, it was possible to check the reproducibility of the experiments by comparing the results obtained from both the original and loaner ITC instruments.

The repeatability is defined as the variation in the measurements taken over a short period of time by a single experimenter and instrument using the same measurement procedure on the same sample and under the same conditions. On the other hand, reproducibility relates to the agreement of test results with different operators, test apparatus, and laboratory locations. In this study, the only factor that was different in the reproducibility check was the experimental instrument. In this section, the repeatability test is first studied and the reproducibility check is discussed afterwards.

The sample chosen for the repeatability test was POPC:Chol at molar ratio of 75:15 %. The standard measurement procedure was repeated twice on this sample. The concentration of the sample was 19.2 mM and the concentration of octanol:water was 4.0 mM as usual. The temperature of the first run was 45.4°C and the temperature of the second run was 45.3°C. Figure 3.4 displays the plot of $q(N_l)$ for the two separate ITC runs of this sample. The measurements were taken on the same day with the same experimental conditions (the slight difference in temperature is negligible). After the first run, the cleaning procedure was followed, as described in Sec. 2.2.2.4, before starting the second run. Comparing the differences between the two data sets, it is determined that the data reproduce within 6%.

Equation 1.7 was fit to the data of the heat released per mole of injectant, as explained in the previous section. Table 3.2 contains the fitting results of the three parameters for the runs as well as the parameter errors reported for each. The fit values for the two runs are not within the parameter errors of the fits, but

47
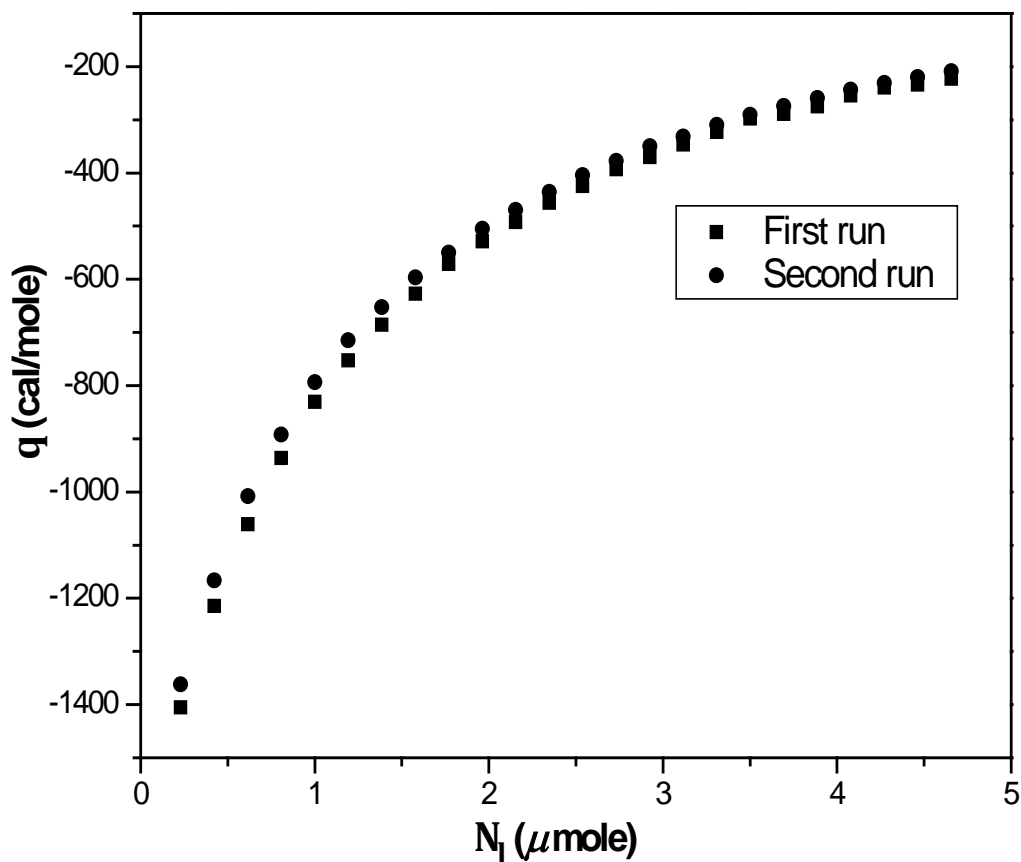
Figure 3.4 **Heat released per mole of injectant data of two separate ITC runs for 25 injections of the 75:15% POPC:Chol sample into suspension of octanol in water solution. The data for the first run is displayed as squares, and that for the second run is shown as circles. The temperatures of the runs were different by 0.1 ℃, which is negligible here. It is determined that the data reproduce within 6%.**

they are consistent. A more reasonable estimate of the parameter uncertainty would be the standard deviation (SD) in these results. Although more runs would have been better regarding the standard deviation calculation, this can still give some idea of the repeatability. Therefore, the standard deviations of the two measurements for each parameter are presented in Table 3.2, as well as the values and relative standard deviations. The standard deviations of K_p, Δh_{int},

and Δh_{dil} are respectively 1%, 5%, 10% of the mean values. These data are presented in the next section as a part of the ITC results for all samples.

ITC run	K_p (mole frac/mole frac)	Δh_{int} (cal/mole)	Δh_{dil} (cal/mole)
1st	7340 ± 40	-1650 ± 17	85 ± 4
2nd	7490 ± 20	-1530 ± 8	72 ± 2
mean	7400	-1590	80
σ	100	80	9
σ/mean	1 %	5 %	10 %

Table 3.2 Values of the partition coefficient K_p, heat of interaction Δh_{int}, and heat of dilution Δh_{dil} obtained from fitting Eq. 1.7 to the data, for two ITC runs of the 75:15% POPC:Chol sample. The mean value from the two fits and the absolute and relative standard deviations are also presented.

As mentioned before, a problem arose with the injection system of the ITC instrument, providing a chance to test the reproducibility of the measurements. The instrument was sent back to the manufacturer and they sent a loaner instrument to the lab to replace the original instrument during the required maintenance. Thus, I was able to compare the results for similar samples using two different instruments. The samples were prepared separately and the experiments were performed at different times.

The ITC measurements were repeated on the two instruments for three different cholesterol molar ratios: 0%, 20%, and 30%. The experimental temperatures of the runs were all set to 45°C, but the exact values reported were slightly different due to the difference in the factors affecting the equilibrium, such as room temperature. Table 3.3 shows the results and standard errors of the fits

to the heat per mole of injectant data for these three samples taken by two instruments. This table also contains the exact values of the experimental temperatures for each run.

ITC instrument	Date	Sample	K_p (mole/mole)	Δh_{int} (cal/mole)	Δh_{dil} (cal/mole)	T (℃)
Original instrument	04/06/2008	Chol 0%	7150 ± 40	-2420 ± 20	130 ± 5	45.2
Loaner instrument	01/08/2008		7170 ± 50	-1830 ± 20	150 ± 6	45.4
Original instrument	11/04/2008	Chol 20%	8100 ± 40	-1280 ±10	48 ± 2	45.3
Loaner instrument	01/08/2008		7370 ± 60	-1310 ±18	70 ± 4	45.2
Original instrument	18/04/2008	Chol 30%	9430 ± 180	-770 ±18	48 ± 5	45.2
Loaner instrument	29/07/2008		7760 ± 90	-575 ± 12	27 ± 3	45.2

Table 3.3   **The fitting results and standard errors of K_p, Δh_{int}, and Δh_{dil} and the experimental temperatures for Chol 0%, 20%, and 30% samples, taken by the original and loaner ITC instruments. All experiments were held at similar experimental conditions by the same observer.**

Except for the measured partition coefficients for Chol 0% sample with two instruments and the heat of interaction for Chol 20%, none of the other parameters for other samples are within the parameter errors reported for the fits in Table 3.3. Table 3.4 displays the mean, standard deviation, and relative SD. There is no visible trend for the relative SD of the measured parameters for different samples. From Table 3.4, we can deduce that the reproducibility of the ITC experiments conducted on different instruments is relatively poor. Nevertheless, because in this study the comparison and trend of the measured

parameters for different samples are more important than the exact values, this fact does not have a significant role in the final results and conclusions of this research. Moreover, measurements from the different instruments are analysed separately, and also in the next sections one of the data sets taken with two instruments will be chosen as the more robust and reliable data.

Sample		K_p (mole/mole)	Δh_{int} (cal/mole)	Δh_{dil} (cal/mole)
Chol 0%	mean	7160	-2120	140
	σ	10	400	10
	σ/mean	0.14 %	20 %	7 %
Chol 20%	Mean	7700	-1300	60
	σ	500	20	15
	σ/mean	6.5 %	1.5 %	25 %
Chol 30%	Mean	9000	-670	40
	σ	1200	140	15
	σ/mean	13 %	21 %	38 %

Table 3.4 **The mean, standard deviation, and relative SD values of K_p, Δh_{int}, and Δh_{dil} for Chol 0%, Chol 20% and Chol 30% samples, resulted by measurements taken with two instruments.**

3.3 ITC Results for all Samples

The ITC measurements were performed for pure POPC and POPC:cholesterol at different molar ratios at T=45±0.5°C. As explained in the previous section, there were two sets of ITC measurements taken using two different ITC instruments. The first set of measurements to be studied, set A, was taken using the loaner instrument for the samples with cholesterol contents of 0%, 10%, 20%, 30%, 35%. The second set of measurements, set B, was taken

using the original instrument for samples with cholesterol contents of 0%, 15%, 20%, 30% and 40%.

The ITC results of the loaner instrument is discussed first, because these data were taken after I had become more practiced in my experimental technique; therefore, I feel that they are more reliable. The loaner instrument was received by the lab on July 23rd 2008 and was sent back when the repaired original instrument was received on August 18th 2008. The raw ITC CFB data taken by the loaner instrument, set A, for different POPC:Chol mixtures is shown in Fig 3.5. The concentrations of lipid suspensions in water were nominally 20mM, which was achieved within 0.5 mM variation except for Chol 10% sample. However, since the data analysed for determining the fit parameters are the concentration-normalized heat changes, as explained in the previous section, these differences in the concentrations of the samples should not affect the validity of the results. The heat of each injection is equal to the area under the corresponding peak. The results shown in Fig. 3.5 demonstrate that the amount of heat released in each injection decreases as the molar content of cholesterol in the lipid vesicles is increased.

The heat released per mole of injectant data was plotted for every lipid sample, as described in Sec. 3.1. Figure 3.6 shows the plot of the concentration-normalized heat per mole of injectant q as a function of total mole of lipid injected N_l. The fitted lines are the results of fitting Eq. 1.7 to each data, using Eq. 1.16 for $\frac{\Delta N_{sb}}{\Delta N_l}$. The values of the heat released are negative for all samples, confirming the reactions to be exothermic. Also for every curve, the magnitude of

52
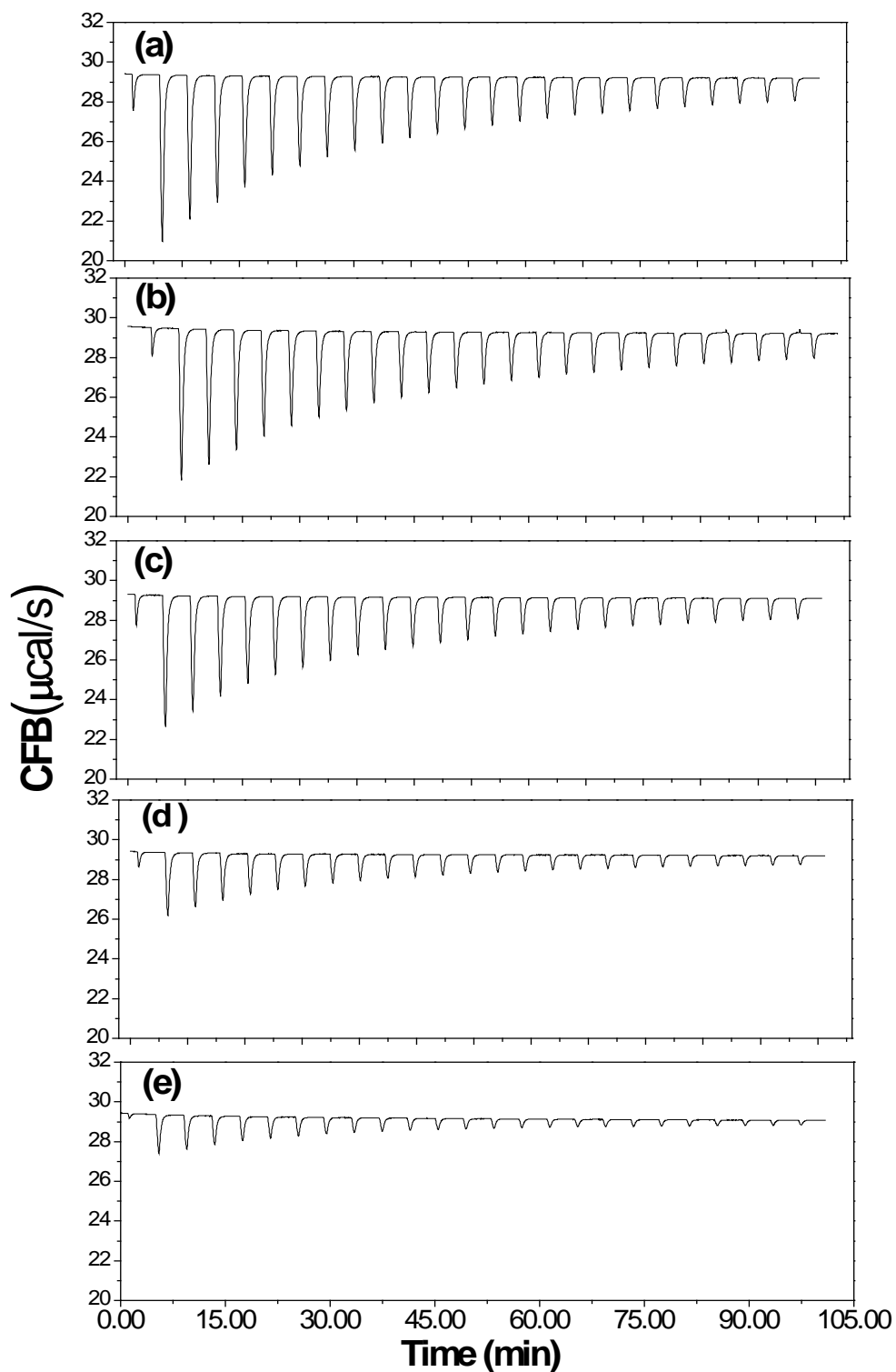
Figure 3.5 **ITC data of set A for 25 injections of lipid vesicles, with different molar ratios, into octanol:water suspension. The lipid samples and their molar concentrations in water are: (a) Chol 0%, 19.1 mM, (b) Chol 10%, 16.4 mM, (c) Chol 20%, 19.8 mM, (d) Chol 30%, 20.1mM, and (e) Chol 35%, 20.5mM. The data was taken using the loaner instrument at T=45°±0.5°C.**

the heat change decreases as the number of injections increase. This is in agreement with the previous discussion of the reduction in the number of free octanol molecules in water after each injection.
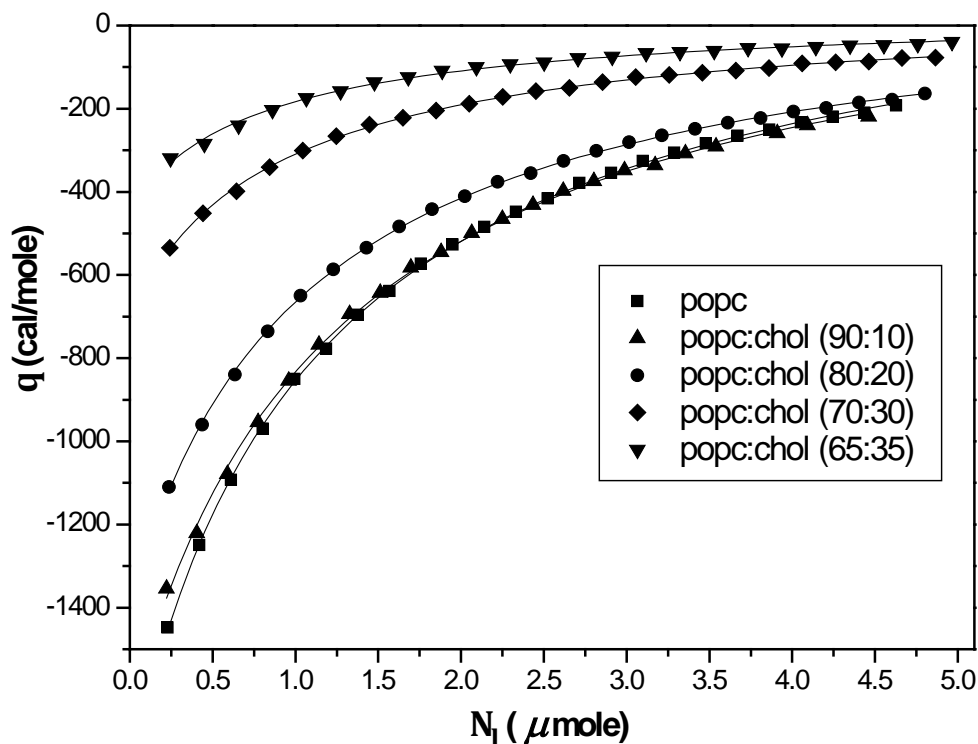
Figure 3.6 **Heat released per mole injectant of data set A as a function of total mole of lipid injected for Chol 0, 10, 20, 30, and 35%. The heats of injections are equal to the area under the corresponding peaks in Fig. 3.5. The curves are the fits of Eq. 1.7 to the data where Eq. 1.16 was used for $\frac{\Delta N_{sb}}{\Delta N_l}$. The values of three parameters, the partition coefficient, heat of interaction and heat of dilution, are determined from the fits and are shown in Table 3.5. The measurements were taken at a temperature of 45±0.5°C.**

The fitting parameters are then determined from the fits for every lipid sample at each different molar ratio. The results of the partition coefficient, heat of interaction, and heat of dilution are plotted as a function of the cholesterol content in Fig. 3.7. The numerical values of the three fitting parameters and their

Figure 3.7 (a) Partition coefficient, (b) heat of interaction and (c) heat of dilution as a function of cholesterol content mole percentage for data set A. The values are determined from the fits in Fig. 3.6 and are listed in Table 3.5. The error bars are the parameter standard errors determined from Origin fitting.

Chol mol%	Date of Exp.	K_p (mole/mole)	Δh_{int} (cal/mole)	Δh_{dil} (cal/mole)
0	01/08/2008	7170 ± 50	-1830 ± 20	150 ± 5
10	14/08/2008	7220 ± 40	-1970 ± 18	110± 5
20	01/08/2008	7370 ± 60	-1310 ± 18	70 ± 4
30	29/07/2008	7760 ± 90	-575 ± 12	27 ± 3
35	06/08/2008	7960 ± 200	-345 ± 16	23 ± 4

Table 3.5 The values for K_p, Δh_{int}, and Δh_{dil} obtained from fitting Eq. 1.7 to the ITC data of set A.

standard errors for different samples are shown in Table 3.5. As it can be seen in Fig. 3.7(a), the partition coefficient values of Chol 0% and 10% are consistent, i.e. within their parameter errors. At higher cholesterol concentration, the partition coefficient values increase, reaching 8000 mol/mol for Chol 35%. The heat of interaction also increases systematically, except for Chol 10% sample, as displayed in Fig. 3.7(b). The heat of dilution decreases constantly with the increasing of cholesterol content in the lipid bilayers as shown in Fig. 3.7(c).

Most of the data taken with the original instrument was obtained before the instrument was returned. The original instrument's injection system was found problematic and the instrument was sent back to the company on 20/07/2008. It was fixed and returned to the lab on 18/08/2008. The samples for this set of measurements were lipid dispersions with cholesterol contents of 0, 15, 20, 30 and 40%. The measurements for the Chol 15% sample, discussed in the repeatability section, were taken after the repair of the original instrument. The experimental temperature was 45±0.5°C, as before. The raw ITC data of the heat released is shown in Fig. 3.8. The plots are on the same scale in order to

facilitate the visual comparison of the peaks' heights for different molar ratios of cholesterol in the lipid dispersion.
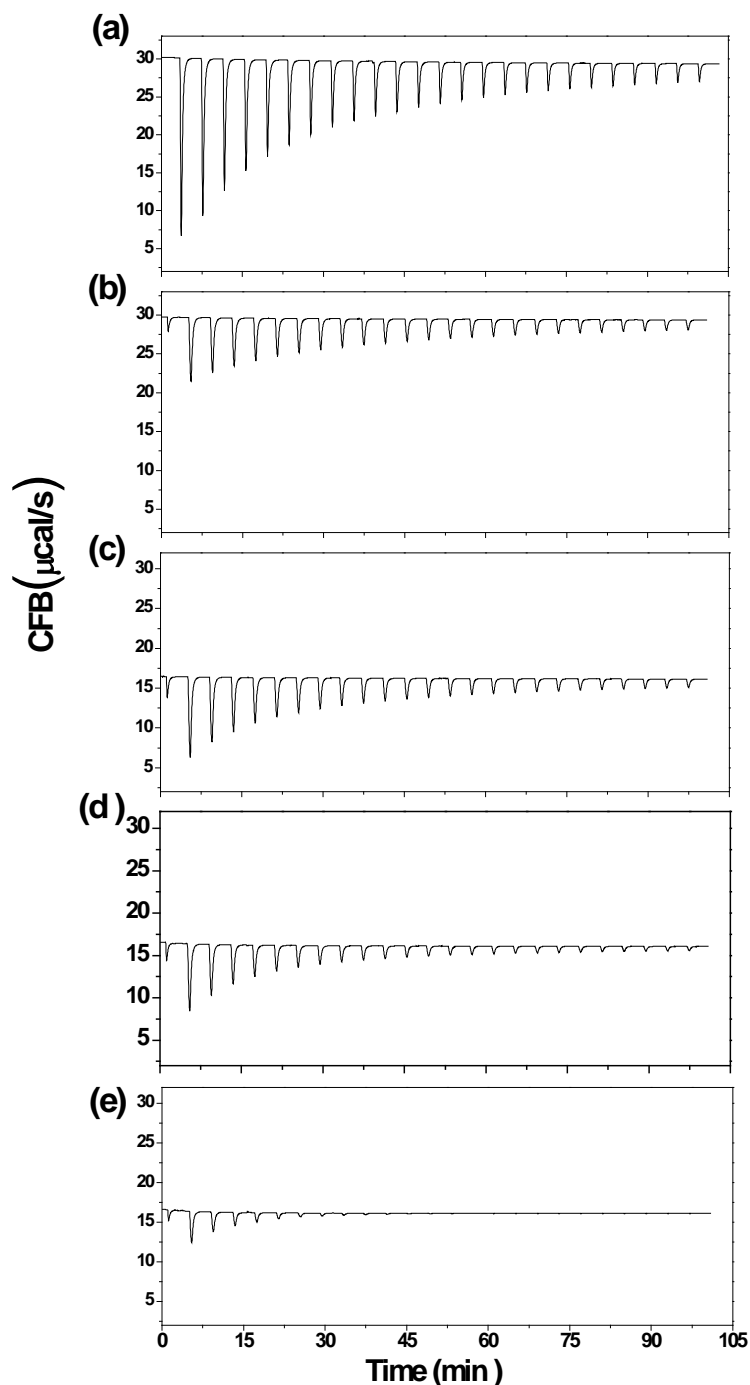
Figure 3.8 **ITC data of set B for 25 injections of lipid vesicles, with different molar ratios, into octanol:water suspension. The lipid samples and concentrations in water are: (a) Chol 0% at 28.1 mM, (b) Chol 15% at 28.4 mM 1st run, (c) Chol 20% at 29.0 mM, (d) Chol 30% at 30.9 mM, (e) Chol 40% at 34.5 mM. The data were taken using the original instrument at temperature of 45±0.5°C. The heat of each injection is equal to the area under the corresponding peak.**

In the measurement for the Chol 0% sample, the injection volume was set to 10 μl for the first peak; therefore, the first peak in Fig. 3.8(a) is not shorter than the second peak like the other plots. This does not affect the results; because, as mentioned before, the data for the next 24 injections are analyzed, excluding the preliminary injection. Another note about these plots is that the baseline for the first two plots is different from those of the next three plots. The baseline is proportional to the temperature difference between the sample cell and reference cell that is kept very close to zero by the instrument after the equilibration is completed. This value can differ according to the temperature of the sample and reference cells and also can be changed by the user. The baseline of the first two samples, Chol 0% and 15% are consistent with all other data taken with the loaner instrument. However, the baseline of the next three measurements, Chol 20%, 30%, and 40%, is different from all other measurements. These three data were taken before the instrument was sent for repair; however, the instrument was working fine at that time and the problem with the injection system arose later. Moreover, the concentration of the samples used was also different , 30±5 mM, because of some miscalculations that were corrected after the measurements were completed. It seems that these data are not reliable due to these significant differences, although they do not affect the heat released values directly because these values are determined from the area under the peaks in the CFB plot and do not depend on the position of the baseline. Therefore, because my proficiency at preparing samples for ITC, working with the ITC instrument and conducting ITC measurements was not fulfilled at the time data

set B was taken, the data set A will be considered as the main result of this study for further discussions and conclusions.

The heat per mole injectant was analyzed as before, in order to determine the fit parameters for different lipid samples. The results of the obtained fit parameters are plotted in Fig. 3.9 as a function of cholesterol content. In the last data point, cholesterol 40%, there is a huge error involved because the heat released values are very small as shown in Fig. 3.8. The data of the two different measurements for the Chol 15% sample are included in Fig. 3.9. Their partition coefficient values were very close, so that the two data points in Fig. 3.9(a) are slightly overlapped and difficult to distinguish. However, the data points in both other plots are completely separate and the differences are distinguishable. The error bars are determined from fitting by the Origin software.

Table 3.6 contains the values of all three fit parameters for different samples. In contrast with the data set A, the change in the partition coefficient is obvious right from the second sample, which is Chol 15%. The ascending trends for the partition coefficient and heat of interaction with increasing of cholesterol content are visible in Fig. 3.9 (a) and (b). The trend for heat of dilution is descending as shown in Fig. 3.9 (c).

Having two different data sets, it would be worthwhile to closely compare the measured partition coefficients and heats of interactions of these two measurements taken with different instruments. Figure 3.10 shows the results of partition coefficient for both sets of data on the same plot for convenience. The first outcome is that both results show ascending trend of partition coefficient with

59

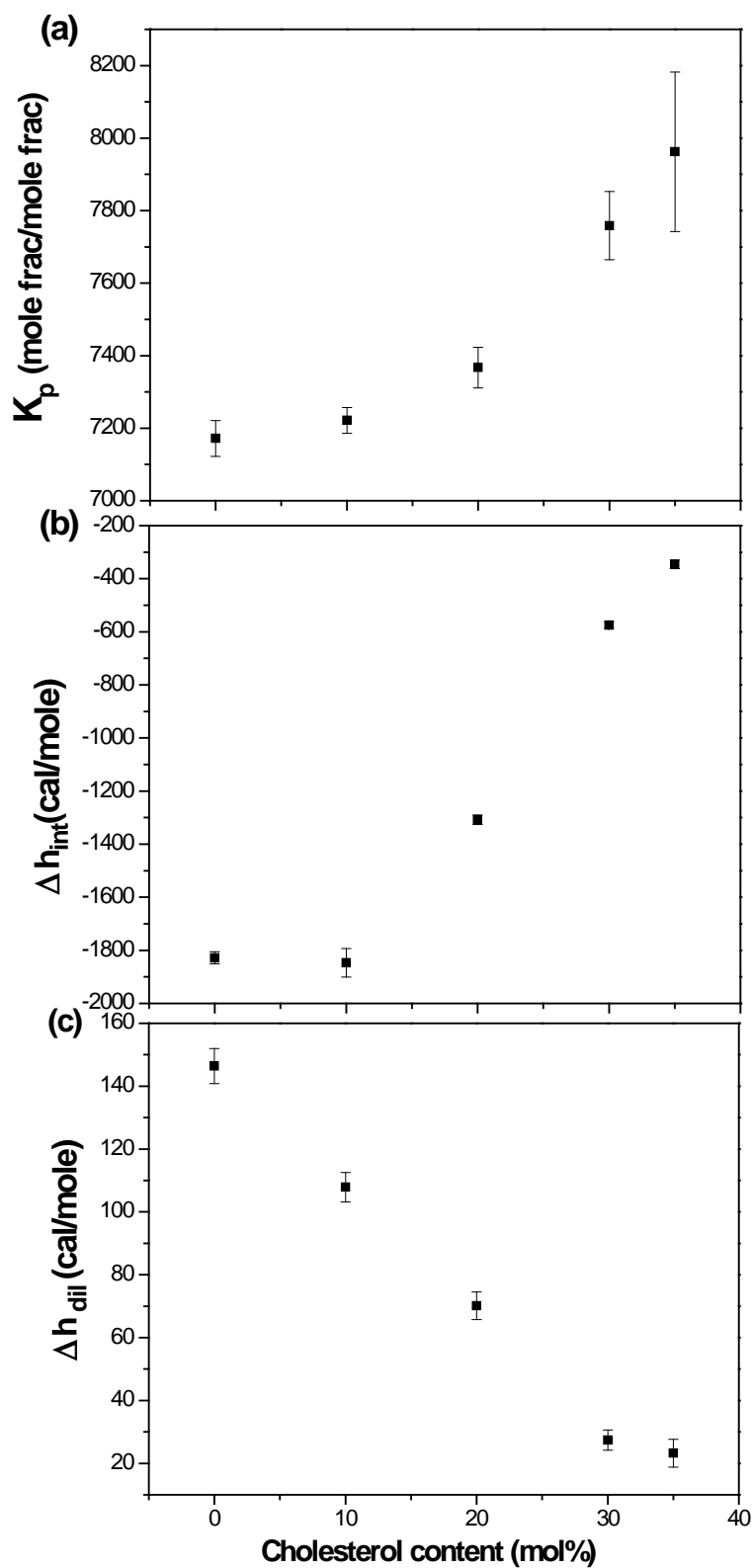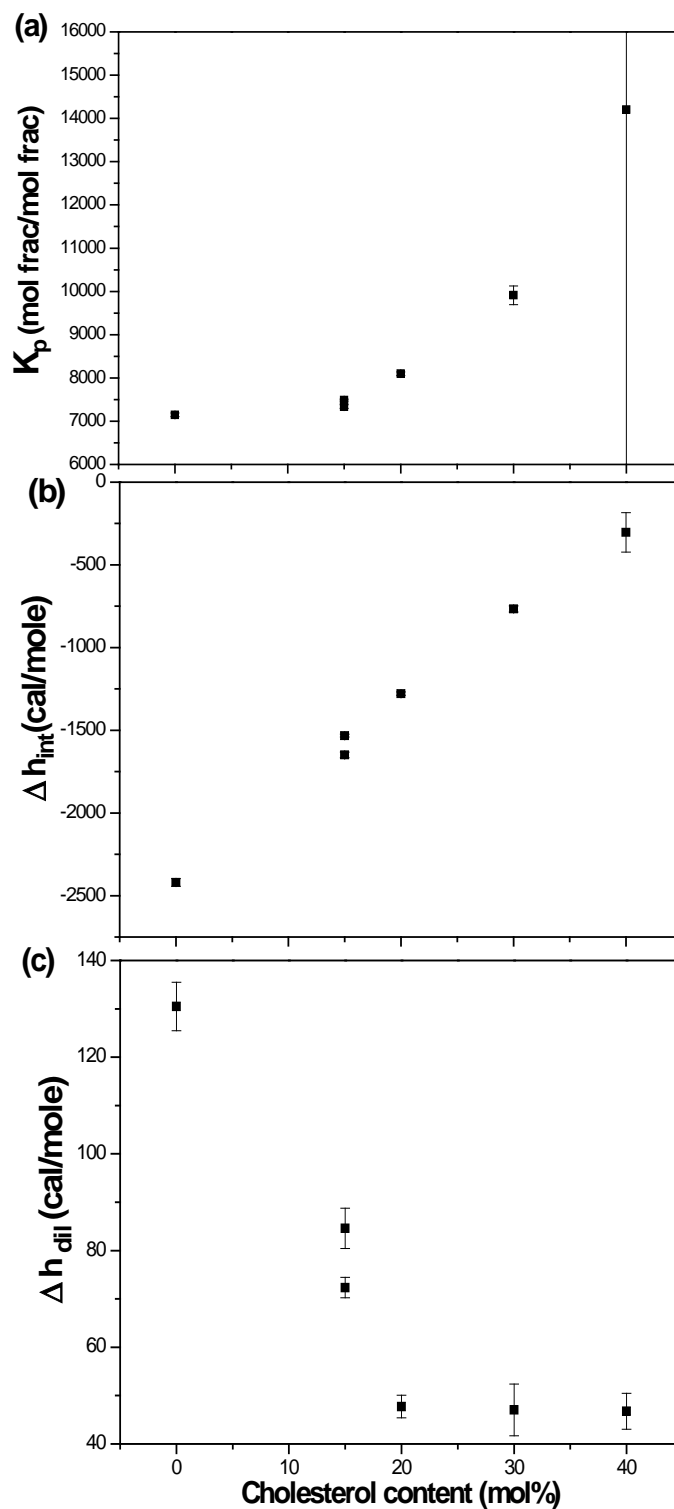**Figure 3.9 (a) Partition coefficient, (b) heat of interaction and (c) heat of dilution as a function of cholesterol content for data set B. The values are listed in Table 3.6. The error bars are determined by Origin from the fitting. The repeatability of the instrument was tested for the Chol 15% sample.**

Chol mol%	Date of Exp	K_p (mole/mole)	Δh_{int}(cal/mole)	Δh_{dil}(cal/mole)
0	04/06/2008	7150 ± 40	-2420 ± 20	130 ± 5
15	26/08/2008	7340 ± 40	-1650 ± 17	85 ± 4
15	26/08/2008	7490± 20	-1530 ± 8	72 ± 2
20	11/04/2008	8100 ± 40	-1280 ± 10	48 ± 2
30	18/04/2008	9400 ± 180	-770 ±18	48 ± 5
40	18/04/2008	14200 ± 13000	-300 ± 120	47 ± 4

Table 3.6 **The values for K_p, Δh_{int}, and Δh_{dil} obtained from fitting ITC data of set B, taken with the original instrument. The last data has very large error due to the small value of the released heat at this molar ratio of POPC and cholesterol.**

increasing of cholesterol molar content in the lipid membranes. As discussed before, the partition coefficient values for Chol 0% of two different data sets are consistent and therefore the corresponding data points are not distinguishable in Fig. 3.10. The Chol 10% and 15% data are single measurements and are not repeated for different instruments. The deviation between different measurements of partition coefficient is visible from Chol 20%, as the second repeated pair of data points. The difference is most significant for the third (last) repeated pair of data points, Chol 30%. The Chol 35% and 40% are measured individually with each instrument. Within the scale of the plot in Fig. 3.10 and according to the higher values of partition coefficient for data set B, the increasing trend is dramatically intensified for the results of the original instrument compared to that of the loaner instrument. The results of set A, the main reported result of this study as discussed before, show rather small but consistent increase in the partition coefficient with increase in cholesterol content. An overall increase of 11% from pure POPC to cholesterol 35% was observed in data set A. Therefore, the increasing trend in the partitioning of 1-

octanol into POPC bilayers with increasing its cholesterol content is sustained in both data sets; however, the relative increase is less in data set A.
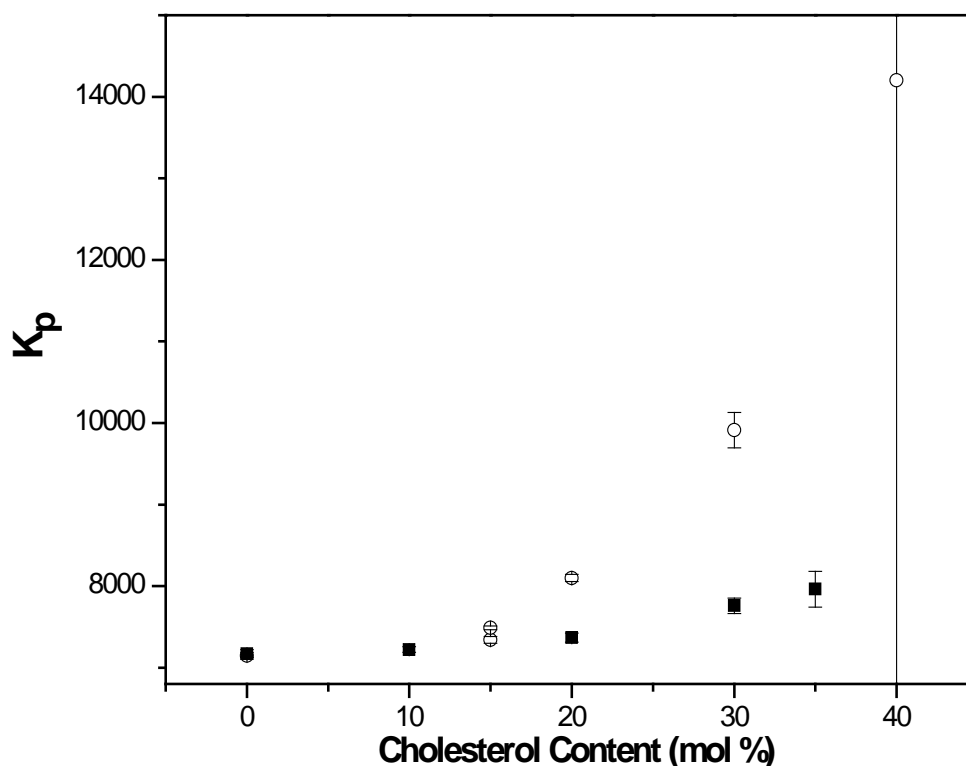
Figure 3.10 Partition coefficients of both data sets as a function of cholesterol content. Data set A, taken with the loaner instrument, is shown in solid squares. Data set B, taken with the original instrument, is displayed in hollow circles. According to the chosen scale for the whole range of partition coefficient values, the data points for Chol 0% of two different data sets are overlapped and not easily distinguishable.

The results of the heat of interaction for both sets of data are plotted on the same graph in Fig. 3.11. The first pair (Chol 0%) shows a significant difference, the second pair (Chol 20%) is almost consistent within the error bars and the last pair (Chol 30%) shows inconsistency. The heat of interaction of set B demonstrates a rather steady ascending trend with increasing cholesterol content. Data set A has also an overall ascending trend except for the first data

point, chol 0%, which is off the increasing trend and that is also the reason it differs from its mate in set B. The overall increase of the heat of interaction from pure POPC to cholesterol 35% in set A is about 81%. It should be noted that since the heat values are negative, when we say there is an increase it means that the heat values become less negative and their absolute value become smaller; therefore, the interaction becomes less exothermic. This seeming conflict with the increasing of partition coefficient will be discussed in Ch. 4.
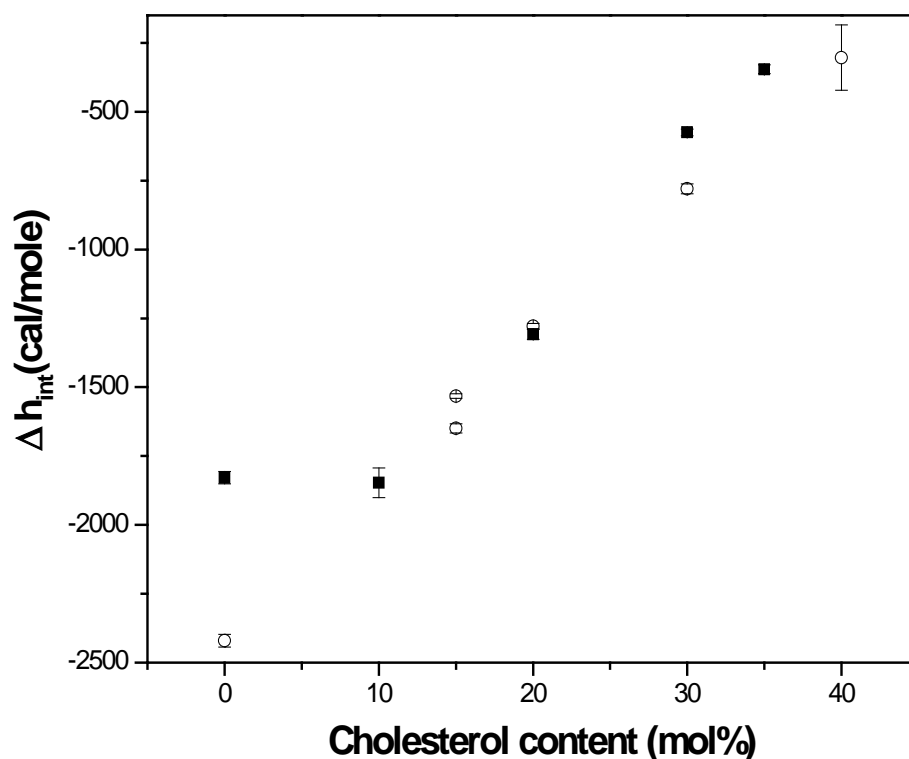
Figure 3.11 Heat of interaction of both data sets as a function of cholesterol content. Data set A, taken with the loaner instrument, is shown in solid squares. Data set B, taken with the original instrument, is displayed in hollow circles.

CHAPTER 4: DISCUSSION

In this chapter we will discuss several aspects of the results. An alternate fitting function, using the same model presented in Ch. 1, will be introduced and the results of fitting this fit function to the ITC data of set A will be compared to our previous results. Moreover, our results will be discussed in the context of similar projects and research conducted by other groups. The heat of interaction and especially the heat of dilution, as the other fitting parameters of the model function used, will be probed in this chapter. Finally, the lipid composition of the biological cell membranes is discussed in this chapter.

4.1   Comparison of Two Fitting Functions for Fitting ITC Data

With the same model presented in Sec. 1.3.2, there is another fitting function developed by Heerklotz [31]. The partitioning model Heerklotz used was formulated for characterizing the thermodynamics of interaction of lipid and detergent. Since it is not important what partitioning is being investigated, the model can be applied to any partitioning problem. The main model function, Eq. 1.7, is the same in both cases but he uses different approximations in the calculation of $\frac{\Delta N_{sb}}{\Delta N_l}$. The fitting function we developed is a generalized form of the Heerklotz function as we did not use any approximation. The Heerklotz function will be discussed below and a comparison of our results with both fitting functions will be presented.

Two important approximations are used in the Heerklotz fitting function. The first one is in the calculation of partition coefficient in terms of the other parameters. The partition coefficient in this model is defined as the ratio of the mole fraction of detergent in bilayer to that in the aqueous subphase [31]. This definition can be restated in our case as the ratio of the mole fraction of octanol in the lipid bilayer to that in water. Other parameters used are also similar and only the notation and symbols are different. For convenience, all the equations of his article are presented in our notation here. In Eq. 1.12, repeated here for convenience,

$$K_p = \left(\frac{N_{sb}}{N_{sb} + N_l}\right) \Big/ \left(\frac{N_{sw}}{N_{sw} + N_w}\right).$$ (1.12)

N_{sb} and N_w are the numbers of moles of solute (in the Heerklotz function: detergent and in our function:1-octanol) in bilayer and in water, respectively. All other parameters are the same in both scenarios. This equation can be simplified as

$$K_p = \frac{N_{sb}(N_{sw} + N_w)}{(N_{sb} + N_l)N_{sw}}.$$ (4.1)

The total number of moles of detergent can be expressed with Eq. 1.13

$$N_s = N_{sb} + N_{sw}.$$

Heerklotz then makes the following approximation: that

$$N_{sw} + N_w \approx N_w;$$ (4.2)

since in a dilute solution the number of moles of detergent in water is negligible compared to the number of moles of water. Moreover, there is a large partitioning

between bilayers and detergent, which leaves even less molecules of deterngent in water as the experiment starts. Using this approximation in the numerator and the substitution of $N_{sw} = N_s - N_{sb}$ in the denominator of Eq. 4.1, yields

$$K_p \approx \frac{N_{sb} N_w}{(N_{sb} + N_l)(N_s - N_{sb})}.$$ (4.3)

Therefore, the number of moles of detergent in bilayer can be determined by solving Eq. 4.3 for N_{sb}:

$$N_{sb} = \frac{1}{2K_p} \left[K_p(N_s - N_l) - N_w + \sqrt{K_p^2(N_s + N_l)^2 - 2K_p N_w(N_s - N_l) + N_w^2} \right].$$ (4.4)

The second approximation is that the number of moles of water is assumed to be constant; whereas in our function we insert the change in total number of moles of water upon injections, by using Eq. 1.11

$$N_w = N_{wo} + n_w V_i.$$

In the Heerklotz function this change in total number of moles of water is neglected due to the small amount of injections (50 μl in their experiments) compared to the total volume of the dilute sample in the cell (1.34 ml). We considered these small changes and used this expression, Eq. 1.11, in our fitting function which contains the independent fit variable N_l, hidden in V_i, as declared by Eq. 1.17.

Now in order to find the change of N_{sb} after an injection of ΔN_l moles of lipid into the detergent dispersion, Eq. 4.4 should be partial differentiated with respect to N_l :

$$\frac{\Delta N_{sb}}{\Delta N_l} \cong \frac{\partial N_{sb}}{\partial N_l} = -\frac{1}{2} + \frac{K_p\,(N_s+N_l)+N_w}{2\sqrt{K_p^2\,(N_s+N_l)^2+2K_p\,N_w\,(N_l-N_s)+N_w^2}}\,. \qquad (4.5)$$

This equation can be compared to Eq. 1.16 repeated below

$$\frac{\Delta N_{sb}}{\Delta N_l} \cong -\frac{K_p}{2(K_p-1)} + \frac{2K_p^2\,(N_s+N_l)+2K_p\,(N_w-N_s)}{4(K_p-1)\sqrt{K_p^2\,(N_s^2+2N_lN_s)-N_s^2\,(2N_s\,(N_w-K_pN_w-K_pN_l)+(K_pN_l+N_w)^2}} \qquad (1.16)$$

It can be shown that Eq. 1.16 simplifies to Eq. 4.5 at the limit of $K_p \gg 1$ and $N_w \gg N_s, N_l$; these conditions are consistent for our experimental concentrations and interactions.

Equation 1.7,

$$q = \frac{\Delta N_{sb}}{\Delta N_l}\,\Delta h_{int} + \Delta h_{dil}\,, \qquad (1.7)$$

using Eq. 4.5 for $\frac{\Delta N_{sb}}{\Delta N_l}$, was fit to our ITC data in order to compare the fit quality and results of Heerklotz' fit function to ours. The data set chosen for this investigation is the data taken with the loaner instrument, (set A), as reasoned in the previous section to be the more reliable data. The heat released data for Chol 0%, 10%, 20%, 30%, and 35% was fit again using Eq. 4.5. Figure 4.1 illustrates the heat per mole of injectant results of both fits for POPC (Chol 0%) sample for a typical comparison. The residuals of the fits are also displayed, demonstrating minor difference between the fits. The fit patterns of the other samples (not shown) and the residual graphs are very similar to the one presented. The residual graphs demonstrate that the difference between the fits for the two fitting

functions is minor for all samples. The fitting parameters for all samples and both

fits are listed in Table 4.1.
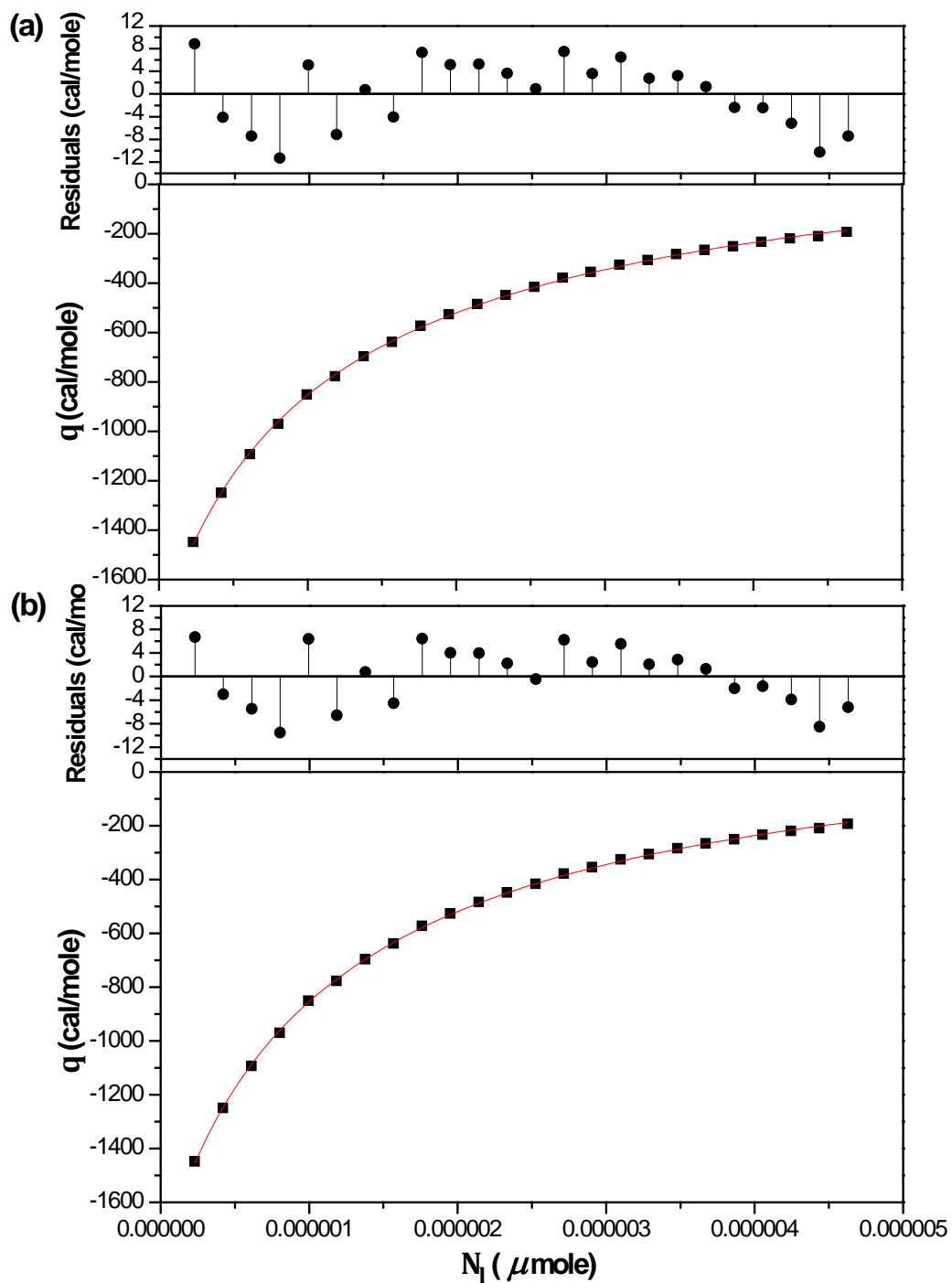
Figure 4.1   Heat per mole of injectant as a function of total mole of lipid injected for POPC sample. Results of fits of (a) the Heerklotz fitting function and (b) our fitting function to the data. The respective residuals are displayed for each fit. The fit results are listed in Table 4.1.

Sample	Fitting function	K_p (mole/mole)	Δh_{int} (cal/mole)	Δh_{dil} (cal/mole)	Reduced Chi-square
Chol 0%	Heerklotz	7370±60	-1820±30	240±8	39.3
	Ours	7170±50	-1820±20	146±6	27.1
Chol 10%	Heerklotz	7430±40	-1970±20	225±6	21.7
	Ours	7220±40	-1970±18	108±5	16.6
Chol 20%	Heerklotz	7560±70	-1300±20	134±6	27.0
	Ours	7360±60	-1310±18	70±4	19.6
Chol 30%	Heerklotz	7900±100	-570±13	55±4	14.7
	Ours	7760±90	-570±12	28±3	12.6
Chol 35%	Heerklotz	8100±200	-340±18	40±5	29.8
	Ours	8000±200	-340±16	23±4	26.9

Table 4.1 The values of K_p, Δh_{int}, Δh_{dil} and reduced Chi-square obtained from fitting Eq. 1.7 using the Heerklotz function, Eq. 4.5, and our function, Eq. 1.16, to the ITC data of set A. The samples were Chol 0, 10, 20, 30, and 35%.

Table 4.1 also contains reduced Chi-square χ^2,

$$\chi^2 = \sum_i \frac{(y_i - y_{fit})^2}{\sigma_i^2} , \qquad (4.6)$$

where y_i is the y-value of each data point and σ_i is the uncertainty of each data

point,

$$\chi_{red}^2 = \frac{\chi^2}{Degree\ of\ freedom} . \qquad (4.7)$$

Reduced Chi-square is an indication of the quality of the fit, since it is minimized

in the iteration process of fitting. Comparing these values between the two fits'

results reveals that the reduced Chi-square of our fitting function is smaller for all samples. Hence, it can be deduced that the fitting function used in this study works better for fitting these data, although only a slight improvement is observed. The partition coefficient values yielded from the Heerklotz fit function are approximately 2-3% higher than those obtained with our function. It is interesting that the heat of interaction Δh_{int} of the two fits is consistent (almost the same) for all samples. It implies that the heat of interaction does not play a significant role in the divergence of these two functions, perhaps because it is the parameter that is multiplied by the expression for the change in the number of moles of lipids upon each injection $\frac{\Delta N_{sb}}{\Delta N_l}$. In contrast, the heat of dilution values, which have been shown to be very sensitive to slight changes, differ for different functions not within the corresponding standard errors. The partition coefficient yielded from two fits for all samples is plotted in Fig 4.2 as a function of the cholesterol content. The results from the Heerklotz fitting function follow the general trend of the results found using our fit function. The partition coefficient of octanol into POPC membranes increases as the cholesterol content is increased for both fits. However, as discussed above our function is more generalized and also shows a slightly better fitting quality based on the reduced Chi-square concept.
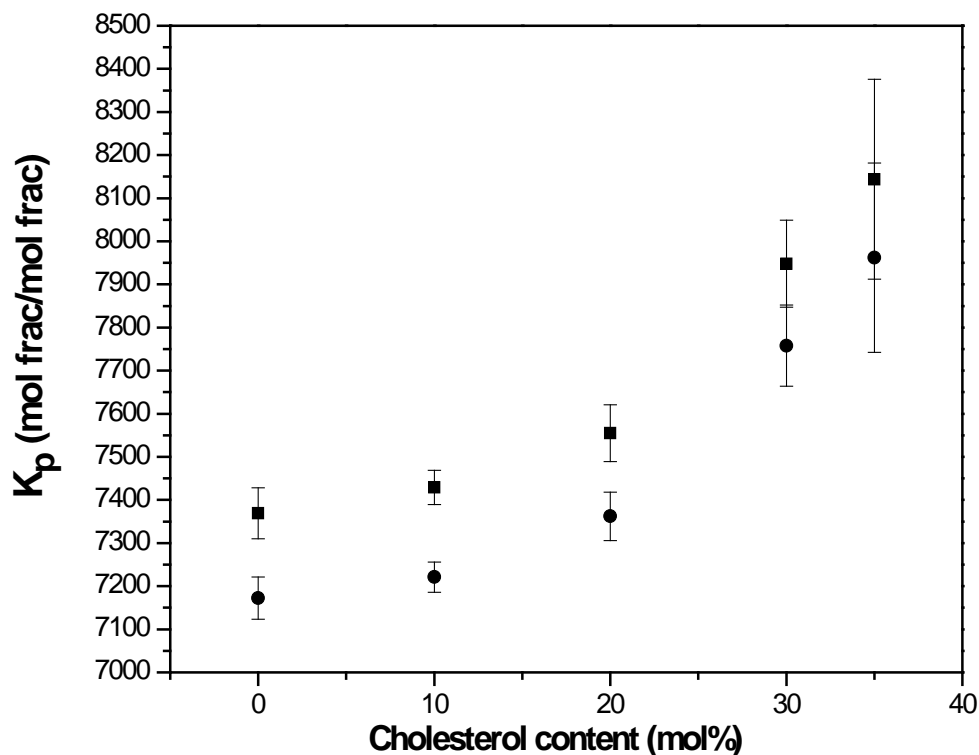
Figure 4.2 **Partition coefficient results of both fits as a function of cholesterol content. The data points displayed in squares and circles are results of the Heerklotz and our fitting functions, respectively. Error bars are the standard parameter errors of the fits. Results of the fit of the Heerklotz function are 2-3% higher than those of ours.**

4.2 Previous Studies of the Interaction between n-Alkanols and Lipid Membranes Using Titration Calorimetry

4.2.1 A Quick Review

The development of calorimetry tools has facilitated the studies of the binding and partitioning interactions of different materials and lipid membranes. In 1992, Zhang and Rowe [32] measured the partition coefficient of n-butanol (C_4H_9-OH) into DPPC bilayers and found its temperature dependence. The partition coefficient starts from 70 at T=15°C, where lipid membranes are in gel phase, to 184 at T=55°C, where lipid membranes are in liquid crystalline phase.

In addition, the partition coefficient of n-hexanol (C_6H_{13}-OH) into DMPC membranes was found to increase from 1255 to 2533 with increasing the temperature from 20°C to 40°C [33].

Trandum, Westh et al [34-38] have investigated alcohol-membrane interactions by means of isothermal titration calorimetry since 1998. In 1999 [35,36], they reported the effect of three short-chain alcohols, ethanol (C_2H_5-OH), 1-propanol (C_3H_7-OH), and 1-butanol (C_4H_9-OH) on lipid bilayers using ITC. The lipids probed were DMPC liposomes in both pure state and mixed with different amounts of sphingomyelin, cholesterol, and ganglioside (GM_1) at temperatures above and below DMPC's main phase-transition temperature. At all temperatures they found that the chemical affinity, the force of attraction, of the alcohols for the lipid bilayers decreases with increasing the chain-length from ethanol to 1-propanol and 1-butanol. The partition coefficient however increases as the chain-length increases; hence, the partition coefficient of 1-butanol is found to be the largest and that of ethanol, the smallest. This is because the large partitioning of solute into the lipid bilayers can occur even with weaker binding affinities, due to the enhancement of the hydrophobic effect compared to the less favourable alcohol-bilayer association for the longer-chain alcohols. They also found that the interaction of short-chain alcohols with lipid membranes is endothermic at the main phase-transition temperature of DMPC and the temperatures above and below that. These interactions strongly depend on the lipid bilayer composition. Lipid bilayers with higher concentrations of cholesterol demonstrate lower binding

enthalpies of ethanol and bilayer, while the opposite is true for the DMPC-ceramide compositions.

Moreover, Trandum et al [37] found that cholesterol increases the affinity of ethanol for DMPC bilayers in the low concentration regime (<10 mole%), whereas the opposite is true for the high concentration regime (>10 mole%). The partition coefficient peaks at about 10% cholesterol mole content; it decreases approximately by a factor of 1.4 from Chol 10% to Chol 0% and decreases approximately by a factor of 6 from Chol 10% to Chol 40%. They also investigated partitioning of ethanol into lipid membranes over a wide range of temperatures (8-45°C), revealing that the partitioning coefficient also peaks at the main phase-transition temperature of DMPC. The peak in the partitioning coefficient with temperature significantly flattens out with increasing cholesterol content.

4.2.2 An In-depth Review of a Comprehensive Study of Partitioning of Different Alcohols into Vesicles of Different Lipid Composition

Rowe et al [39] carried out a very comprehensive and thorough study of the interactions of different long-chain 1-alkanols with different lipids with various headgroups and degrees of unsaturation. They measured the partition coefficients of 1-hexanol (C_6H_{13}-OH), 1-decanol (C_7H_{15}-OH), 1-octanol (C_8H_{17}-OH), and 1-nonanol (C_9H_{19}-OH) into DPPC multilamellar vesicles by means of titration calorimetry. They prepared the multilamellar vesicles by repeating 10 extrusions of the lipid solution through two 400 nm filters. They did not perform the last extrusion step that we did in order to obtain unilamellar vesicles.

73

Their results confirm that the partition coefficient of alcohols into lipid membranes increases significantly with increasing chain-length of n-alkanol, from 839 for 1-hexanol to 55,500 for 1-nonanol. Moreover, they determined the partitioning of 1-octanol into different saturated and unsaturated lipids, DPPC, DLPE, DOPG, DOPC, and SAPC. Table 4.2 contains the partition coefficient values of 1-octanol into these lipids at 45°C. This table also includes the number of double bonds for each phospholipid. It can be deduced from the first three partition coefficient values for three lipids with the same headgroup, that the degree of unsaturation may slightly increase the partition coefficient of 1-octanol. Assuming a uniform trend for this increase, the partition coefficient of a Phosphatidyl Choline with one double bond, such as POPC, is expected to lie in the range $1.81 - 1.98 \times 10^4$, which can be compared to the corresponding value we found 0.7×10^4. These values are of the same order of magnitude although the values appear to differ significantly. This difference may be due to the fact that Rowe et al used a different titration calorimeter instrument, the Microcal's OMEGA.

Lipid	Number of double bonds	K_p
DPPC	0	1.81×10^4
DOPC	2	1.98×10^4
SAPC	4	2.12×10^4
DLPE	0	1.19×10^4
DOPG	2	1.29×10^4

Table 4.2   Partition coefficient values of 1-octanol into different lipids vesicles at 45°C measured by Rowe et al using ITC method, adapted from [39].

In addition, they investigated the effect of cholesterol on the partition coefficient of different alcohols, including 1-octanol, into DPPC bilayers at different temperatures. The range of temperature that was investigated was from 45°C to 60°C and four cholesterol molar ratios (0%, 16 mol %, 19 mol %, and 31 mol %) were studied. This investigation of the effect of cholesterol was conducted only for DPPC and this group performed no study of the effect of cholesterol on the partitioning of alcohols into an unsaturated lipid. As a typical result, the addition of cholesterol at a concentration of 20% was found to profoundly reduce the partition coefficient of octanol into DPPC bilayers at 45°C, by a factor of 2-3. It is discussed in the article that this is due to the effect of cholesterol on the enthalpy of interaction, with a compensating effect on the entropy, resulting in a slight reduction of the free energy. A similar discussion of enthalpy, entropy and free energy pertaining to our measurements is presented in Sec. 4.3.

4.2.3 Conclusion and More Discussion

In conclusion, different groups have studied different aspects of the interaction of various alcohols and lipids. Among these experiments were results reporting that the effect of cholesterol on the interaction of alcohols and liposomes composed of different lipids is to decrease the partition coefficient by a significant factor. However, our results suggest the opposite behaviour, i.e. increasing the partition coefficient when increasing the cholesterol content. Nevertheless, the lipids used in those studies were all fully saturated lipids (DMPC and DPPC), consisting of two saturated acyl chains, while the lipid we

used, POPC, has one mono-unsaturated and one saturated acyl chains. Therefore, there is a possible explanation of this difference due to the different packing abilities of saturated and unsaturated lipids. Since saturated lipids have two acyl chains that are straight, the bilayers containing saturated lipids are tightly packed. On the other hand, unsaturated lipids have either one unsaturated and one saturated acyl chains, or two unsaturated acyl chains. In both cases, the unsaturated chains are bent if there is at least one *cis* double bond, such as POPC. Then, the lipid bilayers consisting of these unsaturated lipids are less packed and they contain void spaces. This picture becomes more complicated when cholesterol is added and the bilayers reconfigure when the cholesterol content in bilayer is increased. Other properties like chain lengths in particular should be considered as well. Therefore, the effect of addition of cholesterol on the partitioning of alcohol into bilayers is a question of configuration of how the gaps are being filled in one case or being expanded in the other.

As discussed in Ch. 1, the addition of cholesterol into phospholipid bilayers universally modulates their fluidity, permeability and thickness. In general, it has been shown that high levels of cholesterol in the membranes reduce the surface compressibility of the bilayers, leading to stiffening of the membrane and increasing its bending rigidity [40-43]. On the other hand, it was found that the membranes containing cholesterol remain fluid and demonstrate resistance to mechanical fatigue [44,45]. Revealing the phase diagrams of lecithin-cholesterol systems [46,47], resolved this paradox; i.e. cholesterol stiffens the membrane while not solidifying it [48]. It was found that cholesterol

broadens the main phase transition of the lipid bilayers and produces an intermediate liquid-ordered phase in between the gel and liquid phases [49]. The phase diagram of DMPC:cholesterol [46], reproduced in Fig. 4.3, is a standard example of a eutectic phase diagram. In an intermediate range of the cholesterol molar ratio below the main phase transition temperature of DMPC, the bilayers are in the coexistence solid-ordered and liquid-ordered phases. Above the transition temperature, the intermediate region of cholesterol mole percent is occupied by the coexistence of liquid-disordered and liquid-ordered phases. For higher cholesterol content at all temperatures the liquid-ordered phase is dominant. The theoretical and experimental phase diagrams of DPPC:cholesterol have also been released [50,51] that are very similar to the one for DMPC.
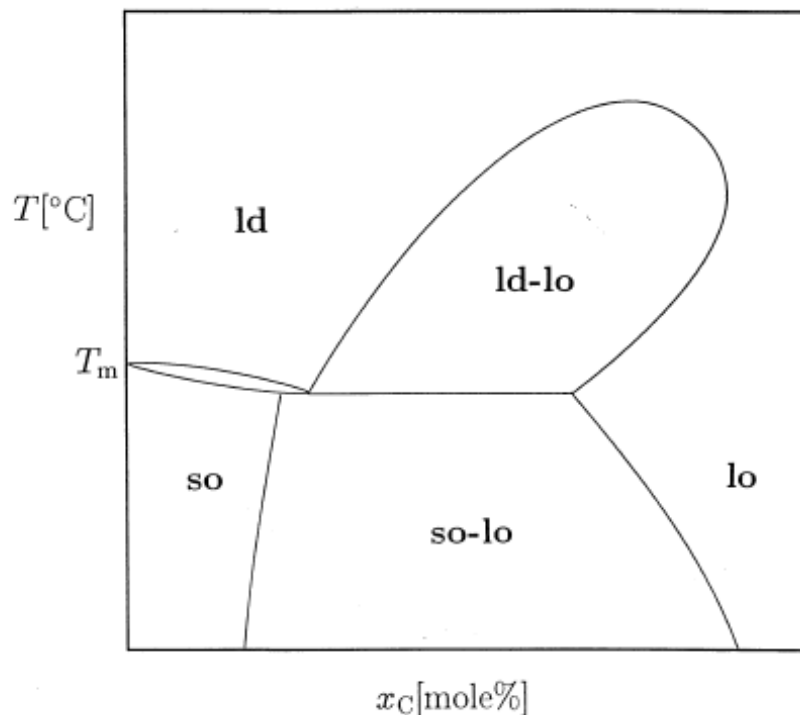
Figure 4.3   Schematic phase diagram for mixtures of DMPC and cholesterol (reproduced from [46]). T_m **is the main transition temperature of pure DMPC. Different phases are labeled as:** *so* **(solid-ordered, the 'gel' phase),** *ld* **(liquid-disordered, the 'fluid' phase), and** *lo* **(liquid-ordered).**

The phase behaviour of POPC:cholesterol mixture has also been investigated [52,53]. Since the phase-transition temperature of POPC is -5°C, the phase diagram of the POPC and cholesterol system mainly resembles the higher part of the DMPC phase diagram. Although the typical phase diagrams reported, Fig. 4.4 and Fig. 4.5, do not completely agree numerically, they are very similar qualitatively. A recent study [54] reports that there is an ld-lo phase coexistence between 15~50 mol% of cholesterol at 45°C, which is also consistent with the results reviewed here.
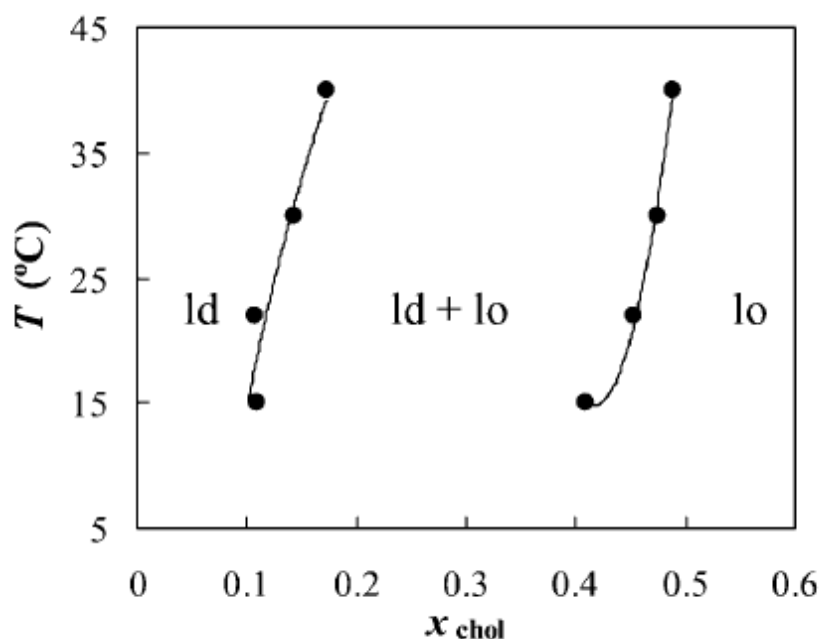
Figure 4.4 POPC/chol phase diagram (reproduced from [52]). The experimental points were determined from <r>DPH and t-PnA lifetime, where DPH stands for diphenylhexatriene and *t*-PnA for trans-parinaric (two fluorescent substances). <r> is the steady-state anisotropy of a probe in a lipidic system whose definition is presented in [52].
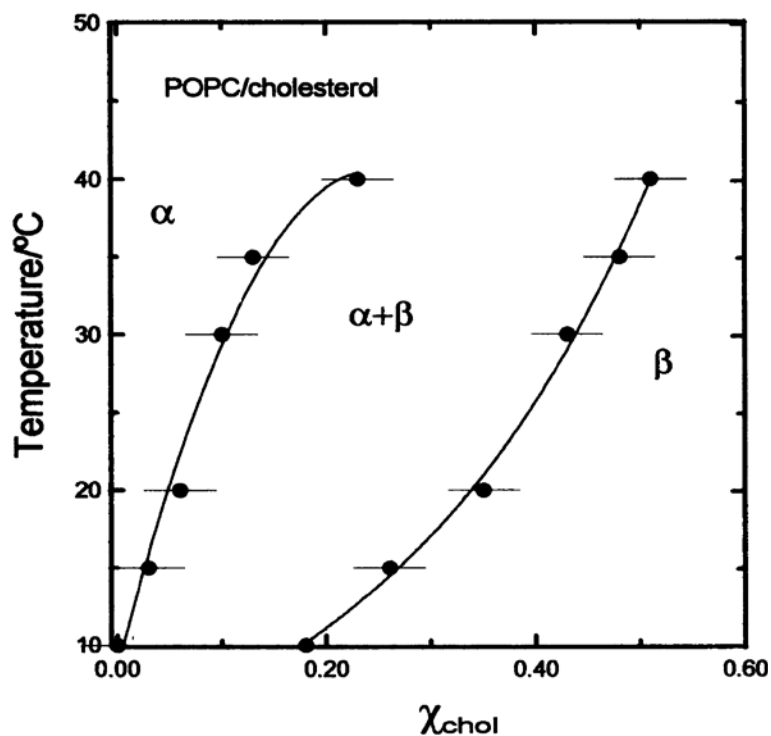
Figure 4.5 The distribution of the α- and β-phases in the POPC/cholesterol system determined from *t*-PnA lifetime analysis (reproduced from [53]). α- and β-phases are the same as *ld* and *lo* phase, respectively.

4.3 The Heat of Dilution and the Heat of Interaction

Although the main goal of this study was measuring the partition coefficient of 1-octanol molecules into the POPC:chol bilayers, the other two parameters of the fit should also be discussed in more detail: the heat of dilution and the heat of interaction.

4.3.1 Additional Heats in a Typical ITC Experiment

In a typical ITC experiment there are other sources of heat that should be considered. Considering component 1 in the syringe and component 2 in the cell, both dispersed in the same buffer, these heats are the heats of dilution of

component 1 and component 2, and also the heat of titrating buffer into buffer which is called the machine blank [26]. In more rigorous conditions, these heats are measured separately and are removed from the raw data. However, since the machine blank and heat of dilution of component 2 are usually very small compared to the total heat changes they are ignored in most cases. The heat of dilution of component 2 can be ignored even if the heat of dilution of that substance in general is large because the injection of 10 μl buffer into a ~1.3 ml cell only affects a dilution of less than one-hundredth [26]. Therefore, in experiments of the type in this study, the placement of lipid dispersion in the injection syringe and alcohol suspension in the cell minimizes the contribution from the dilution heat of alcohol [32,39]. This is important because the heat of dilution of alcohols is rather large while that of lipids is negligible.

The control measurements, also called the blank measurements, for this type of experiment typically consist of: the measurement of heat of dilution for the lipid dispersion by titrating the same sample into water, the measurement of heat of dilution for alcohol by titrating water into the same alcohol suspension used in the experiments, and the blank measurement of the heat of titrating water into water. The last two heats are insignificant, of the order of tens of mcal/mol, and are often neglected [26] with respect to hundreds or thousands of cal/mol of the overall heat changes. These heats were not measured in this study. A more common correction to the raw ITC data is the correction of the dilution heat of the titrant into buffer. According to Heerklotz [55], it may not always be possible to perform a blank experiment that measures the heats of dilution in the absence of

other heat effects. Therefore, it is advantageous to treat q_{dil} as an adjustable parameter in fitting the measured heats per mole q, if no blank measurement was subtracted from the data [56]. We did not measure q_{dil}, but included it in the fitting as explained in Ch. 1.

While no individual experiment was performed for this study to measure the heat of dilution of lipid vesicles dispersions individually, a search in the literature has been made in order to validate our results. We have observed that the heat of dilution from the fit of our model function is different for different cholesterol contents in lipid bilayer. As a result, the heat of dilution of POPC measured by other groups can only be compared to the one for POPC. Our group has also observed that the fit results of q_{dil} is very sensitive to temperature [57]. Thus, this should also be noted for the comparison of our results with others. The most relevant result is the heat of dilution measured by Heerklotz et al [31] using ITC method and the partitioning fit function discussed in Sec. 4.1. They reported the heat of dilution of POPC vesicles at 25°C to be -0.13 kJ/mol = -31.1 cal/mol. The corresponding value of the heat of dilution measured by our group [57] using the Heerklotz fit function is -147 cal/mol, which is significantly larger in magnitude. In summary, the heat of dilution has shown to be very sensitive to slight changes and different fit functions, as can be seen in Table 4.1 where the values of the heat of dilution of the same data are too different for two fits.

4.3.2 Heat of Interaction

In the fitting equation, the heat of interaction is a multiplier of the term containing the partition coefficient. It is the enthalpy evolved on the transfer of the octanol molecules from water to bilayer. This heat is also a very important parameter of the interaction in addition to the partition coefficient and therefore it is worthy of discussion.

The main point that should be made here is about the trend of the heat of interaction for different cholesterol molar ratios. Since the interaction of octanol and lipids in this study is exothermic, it releases heat and the heat values are negative. The heat of interaction (Fig 3.7 and Table 3.5) decreases in magnitude and becomes less negative with increasing cholesterol content. This appears to be in contrast with the increase of the partition coefficient with increasing of cholesterol content in the lipid bilayers. This can be understood by considering the Gibbs free energy of the system.

Based on the definition of the molar Gibbs free energy, at constant temperature we have:

$$\Delta G = \Delta H - T\Delta S \, , \tag{4.8}$$

where ΔG is the change in the molar Gibbs free energy in units of cal.mol^{-1} or J.mol^{-1}, T is the temperature in units of K and ΔS is the entropy change in units of cal.mol^{-1}.K^{-1} or J.mol^{-1}.K^{-1} [58,59]. It can be shown that, at equilibrium,

$$\Delta G = -RT ln K, \tag{4.9}$$

where K is the equilibrium constant, in our case the partition coefficient, and R is the universal gas constant in units of $cal.mol^{-1}.K^{-1}$ or $J.mol^{-1}.K^{-1}$ [33,58,59]. As the partition coefficient increases, according to Eq. 4.9 ΔG becomes more negative. We have observed a positive change in enthalpy. From Eq. 4.8, these imply that the entropy increases so that the −TΔS term becomes even more negative, overcompensating the increase in ΔH. This means that the entropy is increased even more, answering for the interaction being more favorable with increasing the cholesterol content. It should be noted that, since the process is spontaneous and irreversible the entropy change is positive and the change of the Gibbs free energy is negative. This expression is consistent with the fact that the partition coefficient is always larger than one and from Eq. 4.9 $\Delta G < 0$, which is true for reactions that proceed spontaneously [58,59].

An example of a similar trend of partition coefficient and enthalpy in the literature would be the partitioning of detergent octyl glucoside (OG) into DMPC bilayers at different temperatures [60]. Figure 4.6 is a reproduced plot of the heat values of this partitioning at two temperatures of 27°C and 70°C together with the fits. The fitting model used in this study is basically the same as that introduced by Heerklotz. This experiment also shows an increase in partition coefficient K accompanied by an increase in transfer enthalpy ΔH^T, this time as the temperature is decreased implying an increase in entropy.
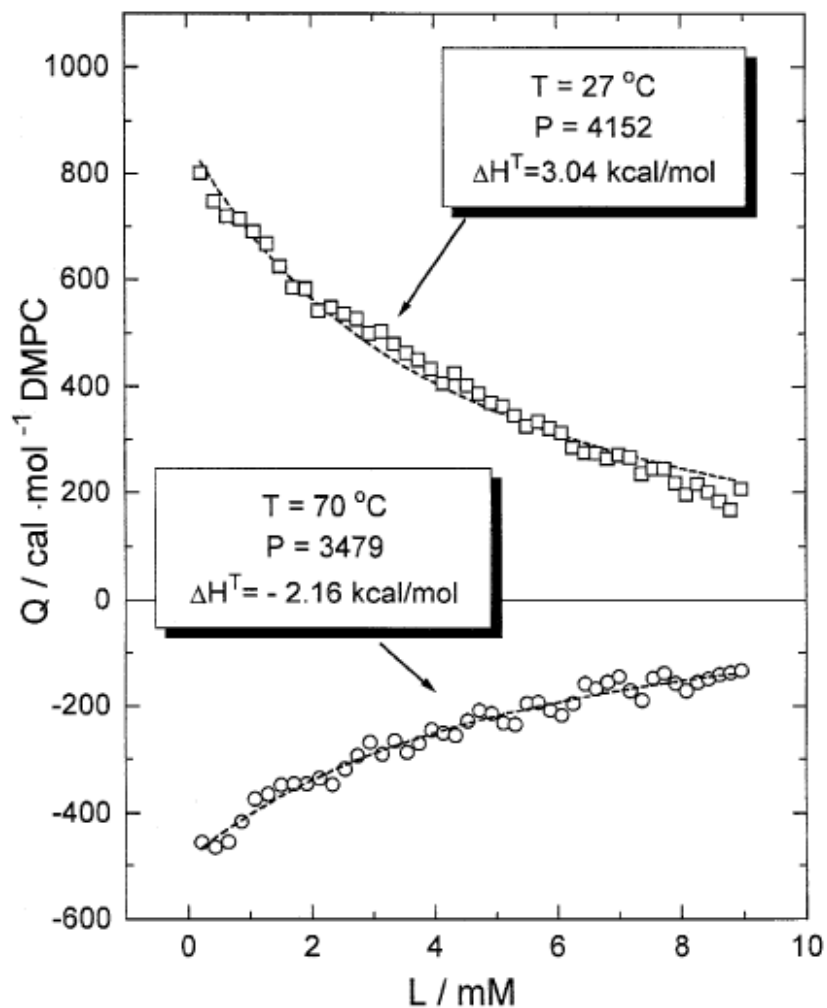
Figure 4.6 **Results of a partitioning experiment of the octyl glucoside (OG) solution and DMPC in the mixed vesicles and surfactant monomers phase [60]. A 3 mM OG solution is titrated with a 50 mM DMPC vesicle suspension. The lines are the fits of Eq. 1.7 with the parameters P, partition coefficient, and ΔH^T, transfer enthalpy, as obtained from a non-linear least square fit.**

4.3.3 The Lipid Composition of Biological Membranes

The reason that phospholipids are commonly used as model membranes

for biological cells is they are the dominant component of the cell membranes.

Table 4.3 shows the weight percentage of different lipids of various biological

membranes. 60% of the membrane lipids of the human erythrocyte (red blood

cell) is made up of phosphatidylethanolamine (PE), phosphatidylcholine (PC), sphingomyelin (SPM), and phosphatidylserine (PS). The human myelin (a neural cell) membrane is 42% phospholipid. The next major component is cholesterol for erythrocyte and it has significant presence in myelin membranes as well. This brief discussion clarifies the motivation behind using the phospholipid-cholesterol lipid bilayers, especially PC-cholesterol membranes, as the model membranes for biological related studies like ours.

Lipid	Erythrocyte	Myelin	Mitochondria (inner and outer membrane)	Endoplasmic reticulum
Cholesterol	23	22	3	6
PE	18	15	35	17
PC	17	10	39	40
SPM	18	8	-	5
PS	7	9	2	5
Cardiolipin	-	-	21	-
Glycolipid	3	28	-	-
Others	13	8	-	27

Table 4.3   The lipid composition of various biological membranes, adapted from [61]. The data are expressed in weight % of the total lipid. The erythrocyte and myelin values are for human sources and the other two are for rat liver. PE, phosphatidylethanolamine; PC, phosphatidylcholine; SPM, sphingomyelin; PS, phosphatidylserine. The dash denotes that there were no traces of the lipid.

Unsaturated phospholipids play a major role in the total phospholipids present in the biological membranes. Table 4.4 contains the concentrations of

the hydrocarbon chains present in the phospholipids of the human red cell, both in weight and molar percent. It should be noted that an unsaturated lipid can have one or two unsaturated fatty acids and therefore the total percentage of the unsaturated fatty acids in a membrane does not necessarily indicate the total percentage of the unsaturated lipids. Since most of the unsaturated lipids, except for sphingomyelin, have one saturated and one unsaturated fatty acid [29], the total percentage of the unsaturated fatty acids in a membrane can be approximated as the total percentage of its unsaturated lipids. This is also backed up by another table [61] which is reproduced in Table 4.5. Table 4.5 shows that the average number of double bonds per phospholipid molecule for most of the metabolically active membranes is larger than one. Therefore, the phospholipids of most of these membranes are unsaturated.

In conclusion, the major lipid component of the biological membranes is made of phospholipids (and cholesterol) and also phospholipids of the more metabolically active membranes are considerably more unsaturated [61]. These are the reasons behind choosing an unsaturated PC together with cholesterol as the model membrane in this study.

Chain length and unsaturation	Total phospholipids (wt %)	Total phospholipids (mol%)
16:0	20.1	22.6
18:0	17.0	17.3
18:1	13.3	13.6
18:2	8.6	8.8
20:0	+	+
20:3	1.3	1.2
22:0	1.9	1.6
20:4	12.6	11.9
23:0	+	+
24:0	4.7	3.7
22:4	3.1	2.7
24:1	4.8	3.8
22:5	2.0	2.6
22:6	4.2	3.7
Saturated	43.9-45.5	45.4-47
Unsaturated	49.9	48.3

Table 4.4   Fatty acid, hydrocarbon, chains in human red cell phospholipids, adapted and calculated from [61]. In the first column, the codes indicate the chain length and number of double bonds, in order. The second column contains the weight percentage of each fatty acid in the total phospholipids present in the human red blood cell, including SPM, PC, PE, and PS, as reported in [61]. The last column is the molar percentages calculated by myself, using the molar weights of each hydrocarbon. The last row includes the total percentages of the saturated and unsaturated fatty acids. The + sign denotes that there were traces of the fatty acid and the concentration detected did not exceed 1%. The concentrations reported do not add up to 100% because other fatty acids with less concentration were not reported.

Membrane	Average number of double bonds per phospholipid molecule
Myelin	0.5
Erythrocyte	1.0
Sarcoplasmic reticulum	1.4
Mitochondria (inner membrane)	1.5
Nerve synapse	>2

Table 4.5   Double-bond composition of phospholipids of various membranes of more metabolically active cells, reproduced from [61].

CHAPTER 5: CONCLUSION

The ITC data analysis of the interaction of 1-octanol with POPC and POPC:cholesterol bilayers at temperature of 45°C reveals that there is a strong partitioning of 1-octanol molecules into the POPC bilayers and that this partitioning increases with addition of cholesterol in the bilayer. Moreover, the heat of interaction becomes less negative as the cholesterol content increases in the bilayer, implying that the entropy change becomes more positive overcompensating this increase. The heat of dilution was found to be lipid-composition dependent and was found to decrease with increasing cholesterol content.

The ascending trend of the partition coefficient as a function of cholesterol molar concentration in the lipid membrane is opposite to that found by other groups for saturated lipids. This implies an important difference between the saturated and unsaturated lipid membranes regarding their interaction with alcohols in the presence of cholesterol. This idea can be investigated and tested by conducting similar measurements for other unsaturated lipids, especially those that are di-monounsaturated such as DOPC or polyunsaturated such as SAPC. The effect of temperature on the partitioning can also be precisely probed using the same method, ITC, or other similar methods, such as differential scanning calorimetry (DSC). Our group has been observed that temperature has

a significant effect on the partitioning parameters of 1-octanol into POPC-cholesterol bilayer [57].

The heat of dilution could also be measured separately, using ITC, in order to check the fit results or to correct the detected heat values and fit the corrected data with only two fit parameters instead of three. However as mentioned before, there are potential difficulties with this approach because of the limitation of performing a blank experiment that measures the heats of dilution in the absence of other heat effects [55]. The other two control experiments that were explained in Ch. 4 could also be measured for a more rigorous study.

Finally, other properties of the POPC-cholesterol vesicles containing octanol, such as their size, mechanical properties, and permeability could be measured in parallel with the partitioning data to complement this project.

REFERENCE LIST

[1]   Wade, L. G., *Organic Chemistry*, 5th ed. New Jersey: Pearson Education, Inc., 2003.

[2]   Tanford, C., *The Hydrophobic Effect: Formation of Micelles and Biological Membranes*, 2nd ed. New York: John Wiley & Sons, 1980.

[3]   Cevc, G., and D. Marsh, *Phospholipid Bilayers*, New York: John Wiley & Sons, Inc., 1987.

[4]   Israelachvili, J., *Intermolecular & Surface Forces*, 2nd ed. London: Academic Press Limited, 1992.

[5]   Small, D. M., ed. *The Physical Chemistry of Lipids (Handbook of Lipid research; v.4),* New York: Plenum Press, 1986.

[6]   Burton, R. M., and F. C. Guerra, eds. *Fundamentals of Lipid Chemistry*, Missouri: BI-Science Publications Division, 1974.

[7]   Henriksen, J., A. C. Rowat, E. Brief, Y. W. Hsueh, J. L. Thewalt, M. J. Zuckermann, and J. H. Ipsen, Universal Behavior of Membranes with Sterols, *Biophys J.*, 90 (2006): 1639–1649.

[8]   Thewalt, J. L., and M. Bloom, Phosphatidylcholine:Cholesterol Phase Diagrams. *Biophys. J.* 63 (1992): 1176-1181.

[9]   Heimburg, T., *Thermal Biophysics of Membranes*, Weinheim: WILEY-VCH Verlag GmbH & Co. KGaA, 2007.

[10] Hille, B., Theories of Anesthesia: General Perturbations versus Specific Receptors, In *Molecular Mechanisms of Anesthesia*, *Progress in Anesthesiology Vol. 2,* ed. Fink, B. R., Raven Press, New York, 1980.

[11] Overton, E., *Studium über die Narkose.* Jena, Germany: Verlag Gustav Fischer, 1901. English translation: Lipnick, R., ed. *Studies of Narcosis*, Chapman and Hall, 1991.

[12] Meyer, H., Welche Eigenschaft der Anästhetica begingt ihre narkotische Wirking? *Naunyn-Schmiedeberg's Arch. Pharmakol.*, 42 (1899): 108-109.

[13] Swenson, R.P., and G.S. Oxford, Modification of Sodium Channel Gating by Long Chain Alcohols: Ionic and Gating Current Measurements, In *Molecular Mechanisms of Anesthesia*, *Progress in Anesthesiology Vol. 2,* ed. Fink, B. R., Raven Press, New York, 1980.

[14] Chin, J. H., and D. B. Goldestein, Effects of Low Concentrations of Ethanol on the Fluidity of Spin-Labeled Erythrocyte and Brain Membranes, *Mol. Pharmacol,* 13 (1977): 435-441.

[15] Suezaki, Y., K. Tamura, M. Takasaki, et al, A Statistical Mechanical Analysis of the Effect of Long-Chain Alcohols and High-Pressure upon the Phase-Transition Temperature of Lipid Bilayer-Membranes, *Biochimica et Biophysica Acta.,* 1066.2 (1991): 225-228.

[16] Griepernau, B., and R. A. Bockmann, The Influence of 1-Alkanols and External Pressure on the Lateral Pressure Profiles of Lipid Bilayers, *Biophys, J.*, 95.12 (2008): 5766-5778.

[17] Zeng, J. W., K. E. Smith, and P. LG. Chong, Effects of Alcohol-Induced Lipid Interdigitation on Proton Permeability in L-Alpha-Dipalmitoylphosphatidylcholine Vesicles, *Biophys, J.*, 65.4 (1993):1404-1414.

[18] Jung, M. E., A. M. Wilson, X. H. Ju, Y. Wen, D. B. Metzger, and J. W. Simpkins, Ethanol Withdrawal Provokes Opening of the Mitochondrial Membrane Permeability Transition Pore in an Estrogen-Preventable Manner, *J. of Pharmacol. and Exp. Therap.,* 328.3 (2009): 692-698.

[19] Tyulina, O. V., M. J. Huentelman, V. D. Prokopieva, et al, Does Ethanol Metabolism Affect Erythrocyte Hemolysis? *Biochimica et Biophysica Acta-Molecular Basis of Disease,* 1535.1 (2000): 69-77.

[20] Colles, S., W. G. Wood, S. Meyers-Payne, J. Joseph, and F. Schroeder, Structure and Polarity of Mouse Brain Synaptic Plasma Membrane: Effects of Ethanol in vitro and in vivo, *Biochemistry*, 34.17 (1995): 5945–5959.

[21] Seeman, P., Temperature Dependence of Erythrocyte Membrane Expansion by Alcohol Anesthetics. Possible Support for Partition Theory of Anesthesia, *Biochimica et Biophysica Acta*, 183.3 (1969): 520-&.

[22] Dubey, A. K., V. A. Eryomin, T. F. Taraschi, e. al, Alcohol Binding to Liposomes by H-2 NMR and Radiolabel Binding Assays: Does Partitioning Describe Binding? *Biophys. J.,* 70.5 (1996): 2307-2315.

[23] Westh, P., and C. Trandum, Partitioning of Small Alcohols into Dimyristoyl phosphatidylcholine (DMPC) Membranes: Volumetric Properties, *J. of Phys. Chem. B,* 104.47 (2000): 11334-11341.

[24] Kawamura H., M. Manabe, M. Myoujou, et al, Partition Coefficients of 1-Alkanols between Water and DDAB Vesicle Membrane Determined by Differential Conductivity Method, *J. of Oleo Science,* 58.4 (2009): 177-184.

[25] Buurma, N. J., and I. Haq, Advances in the Analysis of Isothermal Titration Calorimetry Data for Ligand-DNA Interactions. *Methods,* 42.2 (2007): 162-172.

[26] Ladbury, J. E. and M. L. Doyle, *Biocalorimetry 2, Applications of Calorimetry in the Biological Sciences*, West Sussex, England: John Wiley & Sons Ltd., 2004.

[27] Bouchemal, K., New Challenges for Pharmaceutical Formulations and Drug Delivery Systems Characterization Using Isothermal Titration Calorimetry. *Drug Discov. Today,* 13.21-22 (2008): 960-972.

[28] Chaires, J. B., Calorimetry and Thermodynamics in Drug Design. *Annu Rev Biophys,* 37 (2008): 135-151.

[29] Personal communication with Dr. Jennifer Thewalt

[30] MicroCal Inc. Micro Calorimetry System, User's Manual, http://www.microcal.com.

[31] Heerklotz, H., G. Lantzch, H. Binder, and G. Klose, Thermodynamics Characterization of Dilute Aqueous Lipid/Detergent Mixtures of POPC and $C_{12}EO_8$ by Means of Isothermal Titration Calorimetry, *J. Phys. Chem.,* 100 (1996): 6764-6774.

[32] Zhang, F., and E. S. Rowe, Titration Calorimetric and Differential Scanning Calorimetric Studies of the Interaction of n-Butanol with Several Phases of Dipalmitoyl-phosphatidylcholine. *Biochemistry,* 31 (1992): 2005-2011.

[33] Suuskuusk, M., and S. K. Singh, Microcalorimetric Study of the Interaction of 1-Hexanol with Dimyristoylphosphatidylcholine Vesicles, *Chem. Phys. Lipids,* 94 (1998): 119-138.

[34] Trandum, C., P. Westh, K. Jorgensen, et al, Effects of Ethanol on Liposomes Containing Cholesterol, Sphingomyelin and Gangliosides: a Calorimetric Investigation. *Biophys. J.,* 136 (1998): 207-221.

[35] Trandum, C., P. Westh, K. Jorgensen, et al, Use of isothermal titration calorimetry to study the interaction of short-chain alcohols with lipid membranes. *Thermochimica Acta,* 328: 129-135, 1999.

[36] Westh, P., and C. Trandum, Thermodynamics of Alcohol-Lipid Bilayer Interactions: Application of a Binding Model, *Biochimica et Biophysica Acta-Biomembranes*, 1421 (1999): 261-272.

[37] Trandum, C., and P. Westh, K. Jorgensen, et al, A Thermodynamic Study of the Effects of Cholesterol on the Interaction Between Liposomes and Ethanol, *Biophys J.*, 78 (2000): 2486-2492s.

[38] Trandum, C., and P. Westh, Partitioning of Small Alcohols into DMPC Vesicles: Volumetric Properties, *Biophys J.,* 78 (2000): 328A-328A.

[39] Rowe, E. S., F. L. Zhang , T. W. Leung , J. S. Parr , and P. T. Guy , Thermodynamics of Membrane Partitioning for a Series of n-Alcohols

Determined by Titration Calorimetry: Role of Hydrophobic Effects, *Biochemistry*, 37 (1998): 2430-2440.

[40] Henriksen, J., A. C. Rowat, E. Brief, Y. W. Hsueh, J. L. Thewalt, M. J. Zuckermann, and J. H. Ipsen, Universal Behavior of Membranes with Sterols, *Biophys. J.*, 90 (2006): 1639–1649.

[41] Song, J. B., and R. E. Waugh, Bending Rigidity of SOPC Membranes Containing Cholesterol, *Biophys. J.*, 64.6 (1993): 1967-1970.

[42] Needham, D., and R. S. Nunn, Elastic Deformation and Failure of Lipid Bilayer Membranes Containing Cholesterol. *Biophys. J.* 58 (1990): 997-1009.

[43] Drew Bennett, W. F., J. L. MacCallum, and D. P. Tieleman, Thermodynamic Analysis of the Effect of Cholesterol on Dipalmitoylphosphatidylcholine Lipid Membranes*, J. Am. Chem. Soc.,*131 (2009): 1972–1978.

[44] Bloom, M., E. Evans, and O. G. Mouritsen, Physical Properties of the Fluid Lipid-Bilayer Component of Cell Membranes: a Perspective, *Q Rev Biophys*, 24 (1991): 293–397.

[45] Finegold, L., *Cholesterol and Membrane Models*, Boca Raton, Fl: CRC Press, Inc, pp 273, 1993.

[46] Ipsen, J. H., G. Karlström, O. G. Mouritsen, H. Wennerström, and M. J. Zuckermann, Phase Equilibria in the Phosphatidylcholine-Cholesterol System. *Biochim Biophys Acta*, 905 (1987): 162–172.

[47] Vist, M. R., and J. H. Davis, Phase Equilibria of Cholesterol/ Phosphatidylcholine Mixtures: ^{2}H Nuclear Magnetic Resonance and Differential Scanning Calorimetry. *Biochemistry*, 29 (1990): 451–464.

[48] Lemmich, J., K. Mortensen, J. H. Ipsen, T. H. R. Bauer, and O. G. Mouritsen, The Effect of Cholesterol in Small Amounts on Lipid-Bilayer Softness in the Region of the Main Phase Transition, *Eur Biophys J*, 25 (1997): 293–304.

[49] McMullen, T. P. W., R. N. A. H Lewis, and R. N. McElhaney, Cholesterol-Phospholipid Interactions, the Liquid-Ordered Phase and Lipid Rafts in Model and Biological Membranes, *Curr. Opin. Colloid Interface Sci.*, 8 (2004): 459–468.

[50] Ipsen, J. H., O. G. Mouritsen, and M. J. Zuckermann, Theory of Thermal Anomalies in the Specific Heat of Lipid Bilayers Containing Cholesterol. *Biophys. J.*, 56 (1989): 661-667.

[51] Sankaram, M. B., and T. E. Thompson, Cholesterol-Induced Fluid-Phase Immiscibility in Membranes. *Proc. Natl. Acad. Sci. USA*, 88 (1991): 8686-8690.

[52] de Almeida, R. F. M., A. Fedorov, and M. Prieto, Sphingomyelin/ phosphatidylcholine/cholesterol Phase Diagram: Boundries and Composition of Lipid Rafts, *Biophys. J.*, 85 (2003): 2406-2416.

[53] Mateo, C. R., A. U. Acuna, and J. C. Brochon, Liquid-Crystalline Phases of cholesterol/Lipid bilayers as Revealed by the Fluorescence of *trans*-Parinaric Acid, *Biophys. J.,* 68 (1995): 978-987.

[54] Y. W. Hsueh and J. Thewalt, unpublished data.

[55] Heerklotz, H., The Microcalorimetry of Lipid Membranes, *J. Phys.: Condens. Matter*, 16 (2004): R441–R467.

[56] Heerklotz, H. H., Thermodynamics of Hydrophobic and Steric Lipid/Additive Interactions, In *Biocalorimetry, Applications of Calorimetry in the Biological Sciences*, ed. Ladbury, J. E. and B. Z. Chowdhry, West Sussex, England: John Wiley & Sons Ltd., 1998.

[57] P. J. Patty, unpublished data.

[58] Hammes, G. G., *Physical Chemistry for the Biological Sciences*, New Jersey: John Wiley & Sons, Inc, 2007.

[59] van Holde, K. E., W. C. Johnson, and P. S. Ho, P*rinciples of Physical Biochemistry,* 2nd ed., New Jersey: Pearson Education, Inc., 2006.

[60] Keller, M., A. Kerth, and A. Blume, Thermodynamics of Interaction of Octyl Glucoside with Phosphatidylcholine Vesicles: Partitioning and Solubilization as Studied by High Sensitivity Titration Calorimetry, *Biochimica et Biophysica Acta-Biomembrane*s, 1326.2 (1997): 178-192.

[61] Vance, D.E. and J. Vance, *Biochemistry of Lipids, Lipoproteins and Membranes*, The Netherlands: Elsevier Science B. V., 1996.